Arabian Journal for Science and Engineering (2024) 49:2857–2885
https://doi.org/10.1007/s13369-023-08603-0

REVIEW ARTICLE-COMPUTER ENGINEERING AND COMPUTER SCIENCE

Mounting RIS Panels on Tethered and Untethered UAVs: A Survey

Ahmad M. Nazar[1] · **Mohamed Y. Selim**[1] · **Ahmed E. Kamal**[1]

Received: 6 April 2023 / Accepted: 27 November 2023 / Published online: 10 January 2024
© King Fahd University of Petroleum & Minerals 2024

Abstract
Unmanned aerial vehicles (UAVs) and reconfigurable intelligent surfaces (RISs) are innovative technologies that aim to enhance the quality of communication in next-generation networks. These technologies are individually tailored to specific applications and have demonstrated impressive results. UAVs are known for their flexibility and ease of deployment, while RIS can adapt to changing environments by altering the traditional propagation and reflection schemes. Recent research has combined these two technologies for various applications, improving communication and data transmission in next-generation networks. This paper surveys recent advancements in using tethered and untethered UAVs and RIS in 5G/6G networks. The main objective of this survey is to inspire further solutions that support RIS-assisted UAVs and to provide insights not covered in published UAV–RIS surveys. The survey summarizes how UAVs and RIS can be used to address communication issues. Two case studies are presented to further illustrate this integration's potential benefits. The first case study demonstrates a UAV mounting an RIS to mitigate the impact of base station fronthaul failure. The results suggest that co-locating tethered UAVs with a selected number of base stations can proactively restore any failed fronthaul links. The second case study explores the 3D trajectory of the UAV and the phase shift design of the RIS based on the number of RIS elements and height placement of the UAV. The study considers an untethered UAV with a terrestrial RIS and shows that the propulsion energy of the UAV can be reduced by changing and adjusting the height of the UAV.

Keywords Reconfigurable intelligent surfaces · Tethered UAVs · Untethered UAVs

1 Introduction

The future of data transmission and communication networks is growing tremendously. New modalities for transmitting data emerge, providing a greater field of research for scholars and experimenters everywhere. The notable increase in data exchange and bandwidth annually is of great importance. Maintaining efficient, steady, and successful data transmission arises as a need, along with consistent speeds and interference interception. RIS is a new technology with a low-power meta-surface and electronically manipulated elements properties [1, 2].

RIS shows potential in improving communication and data transmission in wireless networks. The electronically controllable array elements on the RIS can pave new solutions within communications and data transmission. These devices are flexible in positioning and can be placed and attached to any surface, such as buildings and vehicles. RIS array elements can adjust an electromagnetic signal's absorption, phase, reflection, and refraction in any desired direction in real time [3]. With low power consumption and easily manipulated array elements, the channel gain of any incoming signal is maximized for optimal phase and amplitude and sent toward the intended destination. The advantage of utilizing various duplex modes, such as half- and full-duplex modes, supports using an RIS, along with the smart signal interference mitigations within the technology [3, 4].

RIS is a flexible technology that can be merged with other technologies. Unmanned aerial vehicles (UAVs) are autonomous and can be equipped with antennas to provide base station (BS) functionality. These UAVs have a

Ahmad M. Nazar and Mohamed Y. Selim have contributed equally to this work.

✉ Mohamed Y. Selim
myoussef@iastate.edu

Ahmad M. Nazar
amnazar@iastate.edu

Ahmed E. Kamal
kamal@iastate.edu

[1] Department of Electrical and Computer Engineering, Iowa State University, Ames, IA 50011, USA

substantial attribute of being low cost in maintenance and deployment and incorporate high degrees of freedom in a 3D space [5]. This degree of freedom favors mobility by modifying the global trajectory and positioning to create distinct and optimized line-of-sight (LoS) links with other UAVs or ground BSs. Given the lightweight property of RIS, it can be easily mounted on a UAV.

The emergence of UAVs assisted by RISs provides a pathway for solutions to ongoing communication and data transmission problems. The main advantage is merging the signal-manipulative abilities of the RIS and the high degree of freedom involved with a UAV [6, 7]. The UAV can use intelligent positioning and the RIS to position itself in a dead spot but has a precise reflective angle on the LoS link. Techniques such as machine learning are used in some applications to improve communication [8–10]. As presented in [11], communication links improve as positioning and phase change from the previous location, optimizing future communications.

Some challenges are associated with resource allocation in current and next-generational networks, i.e., 5G and 6G. The authors in [12] discussed the preparedness of 5G networks for drones/UAVs from different perspectives, including mobile-enabled drones and wireless infrastructure drones. That does not imply that UAVs face no challenges when used in these networks. Efficiency and scalability remain an issue, so a thorough analysis of the network and its characteristics are required for a next-generational network solution [3, 11, 13, 14]. The authors in [15] proposed a solution to alleviate the battery and backhaul issues of UAVs by utilizing a tethered UAV to provide backhauling to a set of communication untethered UAVs. In addition, they used another untethered UAV to wirelessly charge the communication UAVs.

There are drawbacks to the merger of the two technologies. UAVs experience strict size, weight, and power constraints (SWaP). UAVs have short battery life. The energy spent to keep the UAV in the air is much greater than the communication and processing power [7]. Rotary-wing UAVs expend power to stay airborne and support themselves in mid-air. A problem with merging RIS and UAV is power consumption. Most of the challenges in propulsion emerge from maintaining stable LoS links with ground stations/users, which are more often blocked by territorial obstacles such as buildings or large objects [11]. There exists a silver lining to adding an RIS; manipulating reflection angles and changing signal phases can optimize the maximum signal power through the mechanics of the RIS with any link. In [11], reflectors change their angle to maintain a consistent and persistent link as the environment changes.

Many mounting modalities exist to support the merger of UAVs and RIS. Some solutions emerged following the SWaP constraints, as mentioned above. The idea of implementing tethered UAVs (T-UAVs) to solve the issue of power consumption has been an area of interest for researchers [16, 17]. T-UAVs have the advantage of a consistent power supply but lack the degree of freedom of untethered UAVs (U-UAV).

Another mounting method is mounting an RIS on a building or object to utilize reflected signals from clear LoS links to the UAV [5]. This method introduces the idea of terrestrial RIS, such as mounting RIS on the facade of a building. Terrestrial mounting opens the possibilities for many UAV-assisted applications [11]. More applications are further discussed in the Background and Case Study sections.

This survey aims to provide information regarding existing solutions that utilize the merger of the two technologies and to show that this has strong potential benefits while considering two different power schemes. These power schemes are tethered and untethered connections to UAVs. There is much room for future work within this research realm, and this article provides some state-of-the-art work that achieved compelling results. This survey fills in the gaps missing by other surveys that present some applications and challenges associated with **U-UAV**$^{\text{RIS}}$ [5, 11, 13, 14], where **UAV**$^{\text{RIS}}$ in general indicates the integration of UAVs and RISs. A comparison of what this survey offers compared to the ones referenced is seen in Table 1.

To our knowledge, this survey is the only one that addressed the UAVs' tethered aspect with RIS. The survey also provides notable examples of channel models where approximate simulation of a realistic environment is considered. Finally, two case studies are presented. The first case study shows the great benefit of utilizing UAV$^{\text{RIS}}$ in mitigating the effect of backhaul/fronthaul failures. The second shows that the propulsion energy of the UAV can be reduced by changing and adjusting the height of the UAV.

Furthermore, this survey paper is presented and broken down according to the following format: Section 2 provides overall background information on untethered UAVs, tethered UAVs, and RIS. Section 3 provides detailed information on merging the two technologies, applications, and techniques. Section 2 presents two case studies regarding fronthaul outage compensation and optimizing UAV's 3D trajectory and RIS phase shift. Section 5 presents some challenges and future directions. Section 6 concludes the survey. A list of acronyms used throughout the paper is shown in Table 2. The survey structure is shown in Fig. 1 to improve the flow of information.

2 Background

The following section provides a brief background on UAV and RIS technologies with some applications. Below is a thorough explanation of the immediate differences between untethered and tethered UAVs and a description of RIS technologies.

Table 1 Comparison of mounting RIS panels on tethered and untethered UAVs: a survey to other surveys in UAV^{RIS} topics

Topics	Addressed in this survey	Addressed in [5, 11, 13, 14]
T-UAVs	Addressed	Not addressed
Applications of U-UAV^{RIS}	Addressed	Addressed
Applications of T-UAV^{RIS}	Addressed	Not Addressed
Differences between U-UAVs and T-UAVs	Addressed	Not Addressed
Channel modeling schemes and Estimation	Addressed	Addressed
Channel model examples	Addressed	Not addressed
Challenges associated with mounting techniques	Addressed	Addressed
Spectrum sharing approaches	Not addressed	Addressed
Visible light communication approaches	Not addressed	Addressed
Detailed limitations on RIS	Not addressed	Addressed

Table 2 Table showing acronyms used in the paper

Table of acronyms	
AIRS	Aerial intelligent reflecting surface
AoA	Angle of arrival
BRnB	Branch-reduce-and-bound
BS	Base station
CFmMIMO	Cell-free massive MIMO
DoF	Degree(s) of freedom
DSgNB	Donor SgNB
EE	Energy efficiency
ER	Energy receivers
FSgNB	Failed SgNB
gNB	Next generation node B
HTA	Heavier-than-air
IR	Information receivers
IoT	Internet-of-things
LoS	Line-of-sight
LTA	Lighter-than-air
MEC	Mobile edge computing
NSgNB	Neighboring SgNB
NOMA	Non-orthogonal multiple access networks
QoS	Quality-of-service
RFEH	Radio frequency energy harvesting
RIS	Re-configurable intelligent surface
SNR	Signal-to-noise ratio
STAR	Simultaneously transmitting and receiving
SWaP	Size, weight and power
SWIPT	Simultaneous wireless information and power transfer
SgNB	Small next-generation node B
T-UAV	Tethered unmanned aerial vehicle
UAV	Unmanned aerial vehicle
U-UAV	Untethered unmanned aerial vehicle
UE	User equipment
VTOL	Vertical take-off and landing

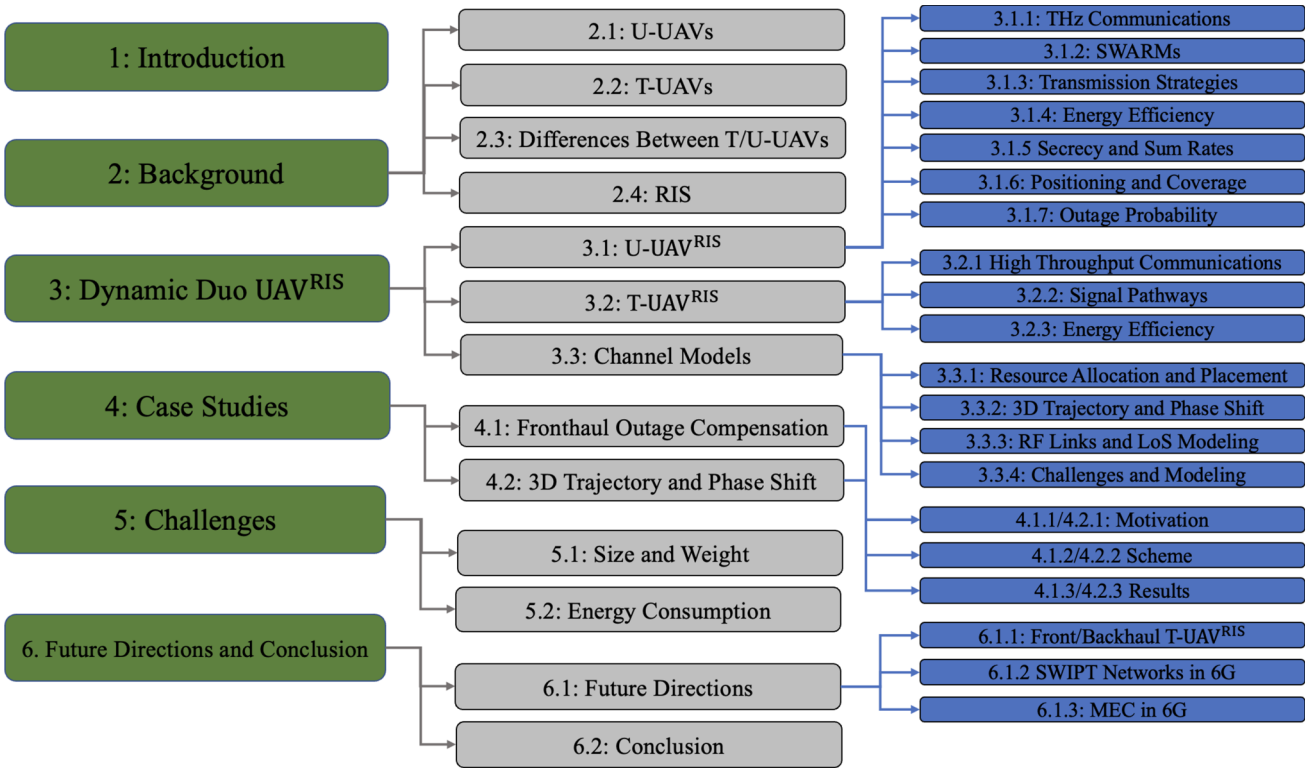

Fig. 1 Structure of the survey and section classification

2.1 U-UAVs

Introducing UAV technology is a favorable idea in the communications and networking field. The high degrees of freedom and low cost of deployment are highly favorable attributes of UAVs [18]. For this paper, there is a distinction between U-UAVs and T-UAVs. U-UAVs deliver communication information and data from senders to receivers by directly sending the payload data. These devices support connection links between base stations, specific nodes, and LoS. The idea is to improve the overall quality-of-service (QoS) within a communication network [19]. The QoS demands can follow a newly paved path to achieving next-generational demand goals using U-UAVs [5].

The use of U-UAVs has potential due to the increase in the likelihood of establishing LoS links and the strong backhaul and access links [5]. In heavy congestion areas, the flexible nature of U-UAVs improves and enhances coverage and quality of service. By staying airborne over these high-congestion areas, UE communication is improved. Some applications that require the above attribute are search-and-rescue and traffic control [20]. These applications depend on the fast deployment and low-cost effectiveness of the data relay provided by U-UAVs.

Another approach that uses a modified and larger-scale version of a U-UAV is seen in [21]. The authors' approach is a High Altitude Platform Station (HAPS) that acts as a computing center in the stratosphere to improve communication for intelligent and connected vehicles. HAPS builds an intelligent transportation systems framework and stores data through an optimized caching algorithm to decrease data transmission propagation delays. The idea of stratospheric deployment increases the coverage area and reachability of the system.

U-UAVs' advantageous property is the dynamic movement and creation of coverage areas [22]. The ability to fly autonomously or have manned flight that creates coverage areas in non-LOS areas makes U-UAVs an alluring deployment item for communication network applications [7, 23]. Different sizes of U-UAVs are used for different missions and deployment criteria; some use even small U-UAVs in swarms to improve data communication and create dynamic LoS nodes [7, 24]. U-UAV swarms and distributed networks promote the abilities of enhanced throughput, scalability, and increased efficiency due to multiple established LoS links [24, 25]. The favorable aspect of the dynamic movement of U-UAVs supports the idea of swarms and allows for efficient resource allocation [24, 25].

Resource allocation is a topic of interest for swarms and distributed joint U-UAV networks. The approach seen in [26] utilizes a two-stage joint hovering altitude and power control in U-UAV networks while considering cross-tier interference

from space-air-ground heterogeneous networks. This joint and distributed approach allows U-UAVs to hover in locations with NLoS links to establish LoS links. The authors' approach improved the network throughput using joint and distributed two-stage tactics while keeping resource allocation in mind [26].

While the favorability of U-UAV use seems convincing, there comes a cost. A U-UAV does not have long battery life [6, 18, 19, 22, 27]. This cost implies that after specific periods, U-UAVs need to recharge. Other constraints include the SWaP constraints. Any extra equipment worth consideration needs to follow the SWaP constraints of a U-UAV to ensure that the U-UAV can support the attached equipment [11]. This downside introduces additional design considerations and protocols to adhere to when attaching UE or aided equipment to a U-UAV; the attribute with the most concern is power consumption. A solution to such a power constraint is the introduction of T-UAVs.

There are multiple types of U-UAVs and multiple applications associated with the type of UAV [22]. The most commonly used types are a fixed-wing U-UAV and a rotary-wing U-UAV [27]. Both have pros and cons; depending on the application, the favored use of one over the other better aids the problem and application. The notable differences between the two most common types of U-UAVs are:

- **Fixed-wing U-UAV:** These U-UAV types are known for their power capacity and coverage area throughout a flight. The disadvantages of fixed-wing U-UAVs are the training requirements and specialized landing zones for any deployment mission [28]. Specialized training is required for liftoff and landing when using this UAV as these procedures do not utilize vertical takeoff and landing as in a rotary-wing U-UAV [6].
- **Rotary-Wing U-UAV:** Compared to a fixed-wing U-UAV, Rotary-Wing U-UAVs require less skill for deployment, and their hovering advantage is strong, especially in autonomous flights. Less skill is required for these UAVs due to their vertical takeoff and landing aspect of flight. The downside is that the power and coverage area is less than a fixed-wing U-UAV [6].

Thorough details of the UAV types and analysis of their multiple aspects can be found in [6, 27, 28].

The recent emergence of a hybrid U-UAV that provides more options for research has been introduced. This hybrid U-UAV, the Vertical Takeoff, and Landing (VTOL), includes the advantages of a fixed-wing and a rotary-wing U-UAV. There have been few approaches involving this hybridized technology, but this technology opens the door to new approaches and solutions to precedent problems [29]. Examples of U-UAVs of the previously mentioned types are shown in Fig. 2 where Fig. 2A is a fixed-wing U-UAV, Fig. 2B is a rotary-wing U-UAV, and Fig. 2C is a hybrid VTOL U-UAV. Table 3 compares the different U-UAV types.

Fig. 2 Types of U-UAVs. **A** fixed-wing U-UAV [30], **B** rotary-wing U-UAV [31], **C** hybrid VTOL U-UAV [29]

One underlying disadvantage shared between all types of UAVs is the flight time due to programming and other constraints associated with components due to battery life [7, 22]. This disadvantage is where T-UAVs come into play to solve the power issue at the cost of degrees of mobility. Each of the mentioned approaches provides a solution with SWaP constraints in mind.

2.2 T-UAVs

Recently airborne communications are attracting great interest from researchers due to their relatively low cost and greater movement range. These airborne communications include different types of flying platforms. Some of them are flying at lower altitudes, such as UAVs. Others fly at higher altitudes, such as high-altitude platforms. However, the main limitation of these flying platforms is the limited flying time. Tethered platforms are introduced to deal with this major limitation [32].

Tethered platforms are attached to a ground station by a heavy-duty cable that gives the flying platform power and fronthauling/backhauling. Although it always sounds uncanny for a flying platform to be tethered, this has some advantages; the most relevant one is the stable power source, allowing unlimited flying time. Tethered platforms are cost-

Table 3 Comparing U-UAV types

Fixed-wing	Rotary	Hybrid
High power capacity	Low power capacity	High power capacity
High coverage	Low coverage	High coverage
One flight mode	One flight mode	Two flight modes
Requires training	Minimal training	Training for mode switching
Slow to deploy	Fast to deploy	Fast to deploy

efficient and have overall low operating costs compared to untethered platforms; however, they suffer from limited mobility.

Tethered airborne platforms fly using static or dynamic lift. For instance, balloons and blimps use static lift, and they belong to the lighter-than-air (LTA) category. The LTA platforms are filled with helium where its density is lower than the density of the air [33].

On the other hand, fixed- and rotary-wing UAVs use a dynamic lift, belonging to the heavier-than-air (HTA) category. The relative motion produces the HTA platforms' lift between the HTA platform and the air. Although fixed- and rotary-wing UAVs are under the HTA category, only rotary-wing UAVs can be tethered, given their ability to hover [34].

Finally, a hybrid category uses both static and dynamic lifts. An example of a hybrid platform is Helikite. It comprises an earth-shaped balloon filled with helium to provide static lift and a kite structure to provide dynamic lift. Combining these two lifts requires less helium than the other LTA platforms. We summarize the main features of all flying platforms that can be tethered, either they are LTA, HTA, or hybrid [32]:

- **Balloons:** are the most used tethered platforms in the LTA category. They are easy to design, manufacture, and deploy with less cost than the other LTA platforms. However, the inflation time of balloons can be an hour or less. They are always deployed in urban areas.
- **Blimps:** or streamlined tethered platforms that can be classified into three categories: (1) tactical, (2) operational, and (3) strategic. The tactical blimps are compact, with a maximum length of 55 feet. The operational blimps are medium-sized with a maximum length of 100 feet. Finally, the strategic blimps are considered the largest tethered platform with a maximum length of 150 feet. The tethered version of blimps is always deployed in urban areas since it must use a mooring launch station.
- **Tethered-UAVs:** Although fixed- and rotary-wing UAVs use dynamic lift and belong to the HTA category, only rotary-wing UAVs can be tethered since they can hover. Tethered UAVs are the fastest to deploy, with a deployment time of within a few minutes. Given its compact size and lightweight, it can be colocated within an SgNB site.
- **Helikites:** belong to the hybrid category; however, they are smaller than balloons; thus, they use less helium (compared to LTA platforms) and use less power (compared to HTA platforms). Helikites can be deployed in dense areas due to their compact size. However, the deployment time may take up to tens of minutes.

Figure 3 shows those, as mentioned above, tethered airborne platforms. Although the transportation method may differ from that shown in the figure, helikites, balloons, and blimps, always require a transportation truck if they are pre-inflated before transporting them to the service location.

Table 4 compares different types of tethered airborne platforms where different factors are considered to compare among them [32, 34].

Based on the different tethered platforms presented in this section and the comparison between them presented in Table 4, the tethered rotary-wing UAVs are the main subject of concern for all cellular network applications that require a tethered platform in a dense area where the platform is tethered to the base station. The T-UAV advantages encouraged well-known companies to test T-UAVs, such as Facebook's Tether-Tenna and AT&T's Flying Cell-On Wings.

2.3 Differences Between U-UAVs and T-UAVs

The following subsection describes the main differences between U-UAVs and T-UAVs at a high level.

- **Deployment and Setup:** T-UAVs are connected to a ground station by a physical link [35]. The tether provides power supply and data communication between the UAV and the BS. U-UAVs operate wirelessly with respect to the BS. They are equipped with onboard batteries and use wireless communication [7].
- **Flight Time:** T-UAVs have extended flight times and receive a consistent power supply so long as the BS remains functional [17]. U-UAVs are constrained by the onboard battery capacity, typically ranging from a few minutes to an hour, depending on the UAV's type, size, and payload [7, 18].

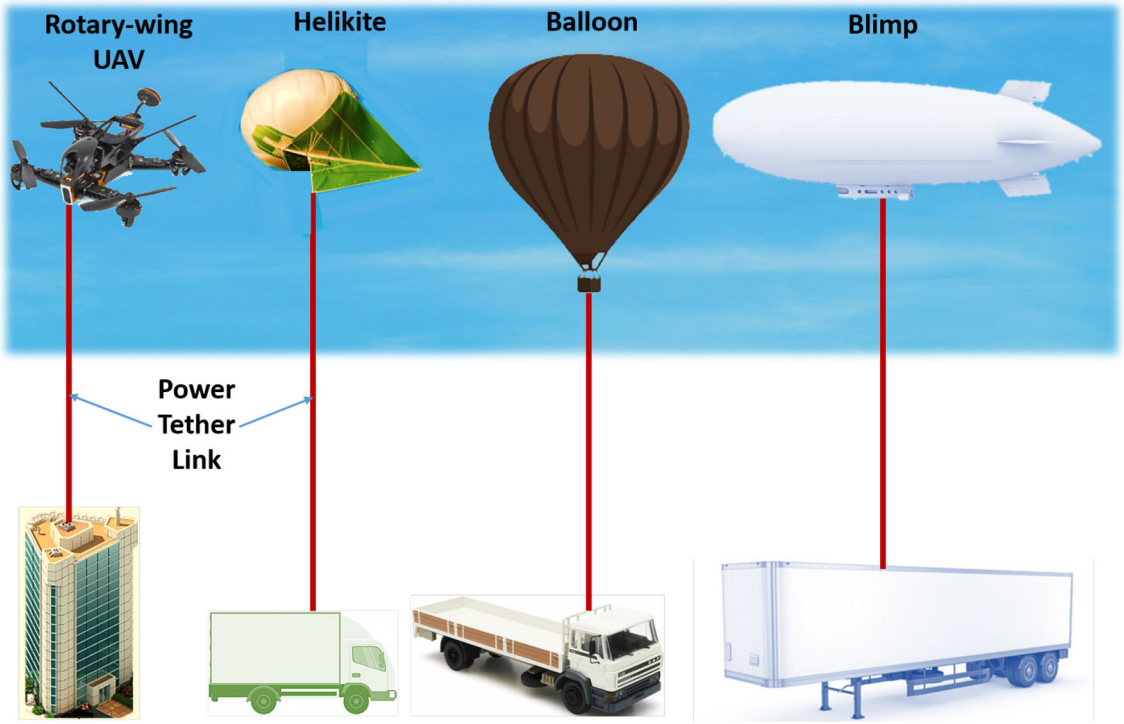

Fig. 3 Tethered airborne platforms

Table 4 Comparing tethered airborne platforms

Properties	T-UAVs	Helikite	Balloons	Blimps
Max. payload	30 lbs	55 lbs	110 lbs	1 Klbs
Max. altitude	150 m	1500 m	600 m	5000 m
Wind speed	35 mph	55 mph	25 mph	100 mph
Fast to deploy	Yes	No	No	No
deployment Personnel	No	Yes	Yes	Yes

- **Payload:** T-UAVs can carry heavier and more sophisticated payloads due to the consistent physical link to the ground station, whereas U-UAVs are often limited by their size, weight, and battery capacity [7, 17, 22].
- **Degree of Freedom and Mobility:** T-UAVs have limited mobility as the length of the tether cable restricts them. They are well-suited for stationary or semi-stationary applications [17]. U-UAVs offer high mobility and flexibility, allowing them to cover large areas and access hard-to-reach locations, making them suitable for various dynamic applications [7, 22, 23].

A summary of high-level differences between T-UAV and U-UAV technologies is seen in Table 5, where the differences are further supplemented by the respective subsections.

2.4 RIS

RIS is a device that utilizes a metasurface that contains cells that consume low power and are electronically manipulated [36]. The low-cost and low-power passive reflection elements provide the backbone of the technology: complete a phase angle change to an incident or reflected signal from a source toward a destination [37]. RIS attempts to maximize the signal-to-noise ratio (SNR) by manipulating the incoming signal's reflection, refraction, phase, and absorption to reflect toward the intended destination. The flexibility of an RIS allows it to adapt to the network and reconfigure itself to optimize the network and communication requirements [37]. RIS was mentioned in one of its first precedent studies in [38], known formally as an electrically tunable impedance surface. These devices were concluded to provide sufficient bandwidth based on their reflectivity concerning how efficient and cheap the development and production of these surfaces are. Another early RIS precedent study is seen in the electronically programmable meta-surfaces in [39]. Here, meta-materials are arranged through a set of scatterers to achieve specific functionality of the material within an area, i.e., programming the scatterers to complete a specific job [39]. Models on transmission and reflectivity are further discussed within [39] along with some simulations explaining the models above. To summarize the main points of this sec-

Table 5 Comparing untethered versus tethered UAVs

Properties	T-UAVs	U-UAVs
X-Hauling	Wired/Wireless	Wireless
UAV type used	Rotary-wing	Rotary-wing, fixed-wing, VTOL
Battery capacity	Consistent power supply	Limited
Ease of deployment	Complex	Fast
Deployment speed	Slow	Fast
Degrees of freedom	Limited	High
Latency	Low latency	Depends
Bandwidth	High	Low
Regulations to follow	Terrestrial and airspace	Airspace

Table 6 Comparison of RIS mounting methods

Active or passive	Mounting method	Movement	Optimization property
Both	Airborne	Dynamic/static	Increases coverage area Due to dynamic altitude
Both	Terrestrial	Static	Optimizes phase angle
Both	UAV	High DoF	Dynamically changes position
		Static/dynamic	Position for optimal Signal transmission
Both	Vehicle	Dynamic	Enhances signal in dead areas

tion, a table concerning the options of RIS mounting methods is shown in Table 6.

RIS is utilized in multiple wireless communications applications. One application is through wireless-aided communications. The RIS reflects incoming signals to improve transmissions by reducing the interference and manipulating the signal's properties [40]. Another application is through information-based transmission. The RIS acts as a modulator and information relayer of RIS-specific data and incoming signal data [40]. These two applications improve communications to a significant degree given a respective approach, with the trade-off being the initial configuration and setup of the RIS [40]. This trade-off opened up a new area of optimizing approaches for SWaP constraints.

The main silver lining of RIS is abiding by a UAV's SWaP constraints. An RIS device's low cost and design make it overwhelmingly advantageous to use in the merger of UAV$^{\text{RIS}}$ communication and networking. Tables 9 and 10 show some specifications for both RIS and UAVs, which are further explained in Sect. 5. This attribute provides a segue into existing mounting techniques for utilizing RIS in communications. The mounting techniques are:

- **Mounting RIS on a UAV:** In some applications, such as in [41], an RIS is mounted on a UAV to manipulate and adjust reflector signal transmission. The UAV's mobility and the RIS's configurability allow for optimal phase change within the high degrees of free mobility.
- **Mounting RIS on Vehicles:** Another possibility for mounting is using manned vehicles to adjust and move the RIS around to establish links with LoS. An example is in [42], where Aerial Intelligent Reflecting Surface (AIRS) is implemented to improve communication. The idea is to achieve higher ground or improve signals in non-LoS areas and strengthen the channel compared to terrestrial mounting methods.
- **Mounting RIS Terrestrial Surfaces:** Some solutions mount RIS devices on terrestrial surfaces [43]. The terrestrial surfaces are chosen based on the locations of the surfaces that optimize signal power and SNR. Examples of such locations are building surfaces or specific ground locations.

Figure 4 displays the above-mentioned mounting techniques. Figure 4A shows vehicular-mounted RIS, Fig. 4B shows UAV-mounted RIS, and Fig. 4C shows terrestrial-mounted RIS on a building.

The smart metasurface cell array elements' manipulative ability makes the technology a convincing choice for optimizing SNR, especially in hotspots or non-LoS areas. For the case of terrestrial mounting, multiple RIS devices can be mounted to determine optimal locations. These locations are determined based on the SNR with the link, BS, or LoS node. Optimizing the reflected signal across the surfaces across determined locations optimizes the overall SNR and improves communication between users and UE in hotspots

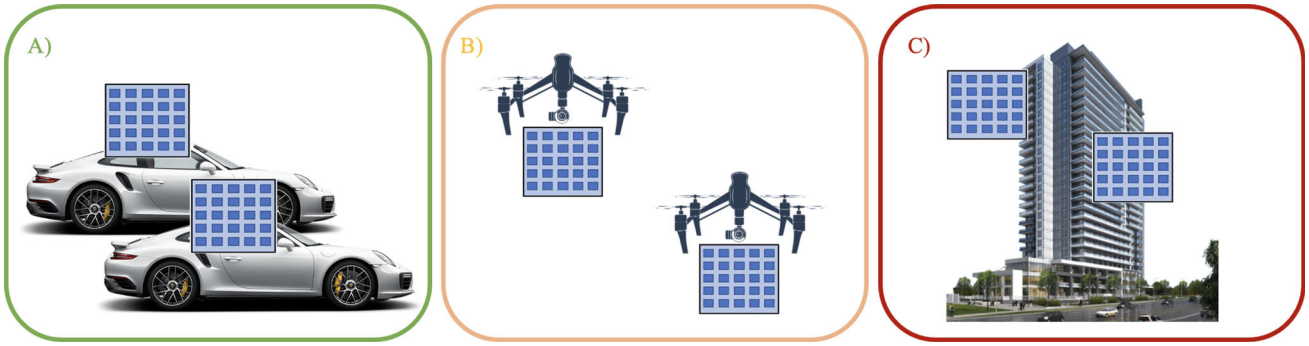

Fig. 4 RIS mounting methods where **A** shows vehicular-mounted RIS, **B** shows UAV-mounted RIS, and **C** shows terrestrial-mounted RIS on a building

and dead locations. As mentioned in [44], a solution involving machine learning, specifically multi-task learning, has been proposed to maximize the overall system throughput and link coverage. The RIS improves wireless communication by redirecting the signal across the most direct path, maximizing the signal power for optimal QoS.

There are two types of RIS devices: active and passive RIS. Both of these models have their pros and cons. The differences are as follows:

- **Passive RIS:** The passive RIS does not amplify an incoming reflected signal and modifies the phase shifts and reflection angles described above. Most available applications and research papers have been completed using passive RIS. According to [1], passive RIS modules are subject to the multiplicative fading effect, which implies that the path loss in the transmitter-to-receiver link is the product of the RIS-to-transmitter and RIS-to-receiver link. The path losses would be equivalent to the sum but not the product. The authors mentioned that the capacity gains of the passive RIS in real-world scenarios are negligible, hence the introduction of the active RIS.
- **Active RIS:** The active RIS amplifies an incoming signal using an amplifier. The amplifier requires power to amplify the incoming reflected signal, implying that active RIS functions at a higher power consumption level than a passive RIS. Some approaches include active RF components on the RIS for further signal processing. An example mentioned in [1] shows an implementation from the authors where a specific amplifier was created to strengthen incident links and achieve a goal of strengthening capacity gains that are negligible in real-world applications of passive RIS. Another application involves an optimization problem in [45] that optimizes the reflecting coefficient matrix at the RIS level and the receive beamforming at the receiver. This active RIS involves improving the spectrum and energy output by using an RIS-aided single-input-multiple-output (SIMO) communication system to improve the amplification gain of the RIS and minimize unintentional noise amplification.

3 Dynamic Duo: UAV^{RIS}

The following section further explains the details of merging RIS and UAV technologies by providing and summarizing findings from precedent studies on UAV^{RIS} papers. The main goal of this section is to provide insight into the advancements made by using a UAV and an RIS together based on different mounting modalities as determined by the problem in the precedent study at hand.

There are multiple mounting methods for UAV^{RIS} technologies. Some of the mounting methods include an RIS mounted directly on a UAV as seen in [46], RIS mounted on a building or terrestrial plane as seen in [47], and RIS mounted on a vehicle [14]. Figure 5 displays four examples of the U-UAV^{RIS} and T-UAV^{RIS} mounting methods for communication between UE and BS in the presence of obstacles to improve communication and data transmission within a network. Figure 5a shows an example of a simple RIS-mounted U-UAV. Figure 5b shows a terrestrial RIS and a U-UAV. Figure 5c displays an example of an active RIS-mounted T-UAV. Figure 5d shows an example of vehicular-mounted RIS and a U-UAV.

In our paper, while we indeed focus on scenarios where RISs are mounted on UAVs, dubbed as our "Dynamic Duo" applications, we also aim to highlight the versatility and broader applicability of RISs beyond just UAV-mounted implementations. For this reason, we have included two additional applications in Fig. 5, namely mounting the RIS on a vehicle and mounting it on the facade of a building. In these cases, the UAVs serve different functions, such as gathering data or providing communication relays, demonstrating the versatility of RIS and UAV technologies.

As for the reasoning and benefits of mounting RISs on UAVs, one of the primary motivations is the enhanced flexi-

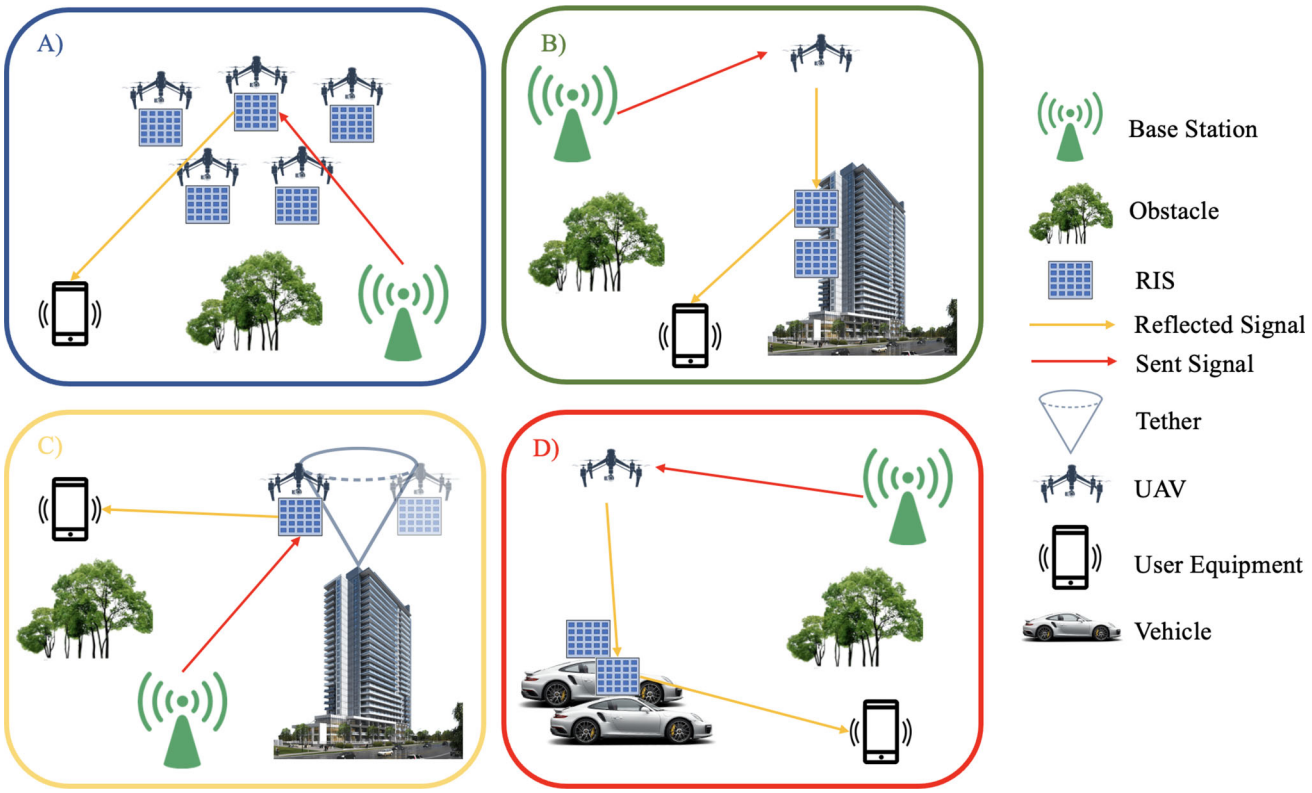

Fig. 5 Four examples of dynamic duo applications **A** U-UAV^{RIS} **B** terrestrial RIS with U-UAV. **C** Active T-UAV^{RIS} **D** vehicular mounted RIS and U-UAV

bility and adaptability this combination provides, which are critical for 6G-enabled communication systems. The UAV's mobility allows for dynamic repositioning of the RIS, aiding in overcoming obstacles or optimizing signal pathways in real time, a functionality that static RIS installations lack.

The survey provides information from various references to support the claims and show the technologies in question. Tables 7 and 8 show references providing information on U-UAV^{RIS} and T-UAV^{RIS}, respectively. The tables present the main topics associated with the references, the mounting methods of the RIS, and the optimization problem solved. Multiple utilities represent more than one method associated with the column header in the tables.

For Table 7, [9, 41, 44, 48–50] show approaches dealing with machine learning. References [24, 45, 47, 50–60] show untethered approaches with multiple parameters optimized in the approach. Untethered aerial approaches are seen in [21, 41, 42, 45, 46, 48, 49, 52, 56–61]. Untethered and terrestrial discussions are seen in [9, 51, 53, 54, 62–65]. Surveys on U-UAV^{RIS} are seen in [5, 11, 13, 14]. Reference [66] presents an ideal hybrid online–offline solution with multiple mounting utilities. Performance analyses on U-UAV^{RIS} are completed in [64, 67]. References discussing maximizing variations of rate parameters for U-UAV placement are discussed in [65, 68].

For Table 8, references [16, 17, 69] discuss tethered approaches with a terrestrially mounted RIS with their respective optimization algorithms. A tethered, aerial approach is seen in [35].

3.1 U-UAV^{RIS}

Many successful precedents use this merger of technologies. The utilization of the merger comes through different mounting techniques. These mounting techniques are aforementioned in the Background section. U-UAVs use the adaptability and configurability of RIS to enhance the SNR and optimize the phase shift of reflected angles [3, 18].

3.1.1 U-UAV^{RIS} in Terahertz Communications

One elaborate example of fully utilizing the advantages of U-UAVs and RIS is in support of terahertz communication as mentioned in [51]. The authors explore improving terahertz communication which suffers from long-distance transmission signal loss. The authors implemented a UAV-assisted RIS device where the RIS is terrestrial, and the U-UAV hovers in locations with no strong downlink connections. The proposed solution helped bypass obstacles and improved communication at the terahertz level due to the degree of

Table 7 Untethered dynamic duo summary

Ref	Main topic	Mounting method	Optimization
[5]	RIS-assisted UAV information	Multiple utilities	×
[9]	3D trajectory and phase shift for U-UAV^{RIS} Using machine learning	Terrestrial	Multiple utilities
[11]	Survey on RIS and UAV	Multiple utilities	×
[13]	UAV^{RIS} Performance and Analysis Survey	Multiple utilities	×
[14]	Vehicular UAV^{RIS} Survey for 6G	Vehicular	×
[21]	HAPS	Aerial	Minimum propagation Delay
[24]	Terrestrial and Aerial RIS versus SWARM RIS	Multiple utilities	Multiple utilities
[41]	Enhancing mm-wave networks Using reinforcement learning	Aerial	Maximize downlink Capacity
[42]	Panoramic signal reflection	Aerial	Maximize SNR
[44]	RIS aerial-assisted communications Using multi-task learning	Multiple utilities	Maximize system Throughput
[45]	Increase signal amplification	Aerial	Multiple utilities
[46]	Estimating AIRS positioning	Aerial	AIRS deployment for UE-BS Comm.
[47]	Joint UAV placement and RIS phase shift Optimization in downlink networks	Aerial	Multiple utilities
[48]	THz communications using deep learning	Aerial	Multiple utilities
[49]	Joint flying RIS trajectory And phase shift design using Deep reinforcement learning	Aerial	Multiple utilities
[50]	STAR-RIS-assisted U-UAV communications	×	Multiple utilities
[51]	U-UAV^{RIS} THz communications analysis	Terrestrial	Multiple utilities
[52]	Energy efficient Air-to-ground networks with U-UAV^{RIS}	Aerial	Multiple utilities
[53]	Joint communication and trajectory Design for U-UAV^{RIS} SWIPT networks	Terrestrial	Multiple utilities
[54]	Wireless power transfer Systems with U-UAV^{RIS}	Terrestrial	Multiple utilities
[55]	Hybrid aerial-ground UAV^{RIS} Communications	Multiple utilities	Multiple utilities
[56]	Consensus-based navigation of UAV^{RIS} For LoS wireless communication with UE in high-density areas	Aerial	multiple utilities
[57]	UAV^{RIS} with MIMO	Aerial	Multiple utilities
[58]	3D trajectory and phase shift design	Aerial	Multiple utilities
[59]	MEC and UAV^{RIS}	Aerial	Multiple utilities

Table 7 continued

Ref	Main topic	Mounting method	Optimization
[60]	U-UAV^{RIS} Secure communications With resource allocation and Jamming	Multiple utilities	Maximize secrecy rate
[61]	Improving EE in Emergencies	Aerial	Multiple utilities
[62]	IRS-enhanced UAV Multi-NOMA networks	Terrestrial	Maximize network Sum rate
[63]	Robust secure UAV^{RIS}	Terrestrial	Multiple utilities
[64]	UAV^{RIS} Decode-and-forward Performance analysis	Terrestrial	×
[65]	UAV^{RIS} Placement and Resource Allocation	Terrestrial	Maximize sum rate
[66]	Hybrid offline–online design for U-UAV^{RIS} Communication	Multiple utilities	×
[67]	Outage performance analysis	Multiple utilities	×
[68]	Enhancing security for U-UAV^{RIS}	×	Maximize secrecy rate

Table 8 Tethered dynamic duo summary

Ref	Main Topic	Mounting method	Optimization
[16]	Aerial BS using T-UAV	Terrestrial	×
[17]	Improving coverage for QoS	Terrestrial	Coverage area
[35]	T-UAV^{RIS} for EE and Reliable communication	Aerial	Average bit error rate
[69]	T-UAV^{RIS} RFEH	Terrestrial	Maximize rate for RFEH

freedom of the U-UAV and the RIS. Given a specific hovering time and a high degree of freedom, the U-UAV hindered the rate of signal loss at long distances with the aid of the configurable RIS that optimizes the signal path. It is seen that the downsides of using the U-UAV are its power consumption and short battery life. With the aid of the RIS, the hovering U-UAV can conserve energy instead of constantly moving due to the RIS configuring its array elements for optimal phase angle and signal propagation.

In another realm of terahertz communication, machine learning can be implemented to learn the optimal location of data reflection from UE to BS. In [48], the authors implement a U-UAV-carrying-RIS solution to solve the path loss disadvantage of terahertz communication. The authors implemented a gated recurrent unit-based recurrent neural network, tracking UE locations and serving beams. The locations were then passed through some computations in the hidden layers in the network, where the output is the optimal location of data transmission with minimal path loss factors of an RIS-carried-U-UAV. While they noted anomalies such as being too close to beams affecting the states and output locations, the performance evaluations favored using the merger of the technologies to improve communication.

3.1.2 U-UAV^{RIS} in SWARMs

Another application of U-UAV^{RIS} is mentioned in [24], where multiple U-UAVs implement RIS-assisted communication by mounting moderate-sized RIS onto U-UAVs. Multiple U-UAVs hover around within a given area, creating a SWARM. Data are collaboratively transmitted at different angles while forming the MIMO channel. This spatially multiplexed channel increases the number of users and the LoS nodes within dead areas. This approach allows for cooperative panoramic full-angle reflection, which constructively adds signals between users and minimizes interference that effectively enhances the signal.

Similarly, another approach mentioned in [62] implements a multiple UAV-assisted RIS network to optimize signal transmission in Non-Orthogonal Multiple Access Networks (NOMA). Multiple UAVs are mounted with base stations to implement a NOMA and provide coverage for many ground users with the assistance of a RIS for optimal signal reflection transmission. The optimization problem solved within this approach is maximizing the network's sum rate through non-convex optimization in a block coordinate descent-based iterative approach. The authors' solution results in a higher overall channel quality, and the flexibility of the UAV and

RIS can further increase the maximum sum rate with the aid of the algorithm mentioned earlier.

The approach in [46] uses multiple AIRS mounted on U-UAVs to estimate the angle of arrival (AoA) for the direct path between UE and the AIRS. This approach estimates the AoA for a given BS using AIRS, where the access point processes data received from the UE and the AIRS. The AoA is based on channel estimation. The authors presented two different methods for estimating the AoA for a multiple AIRS approach, where one method uses an AoA-based positioning algorithm and another uses an angle domain-based AoA estimation algorithm. Both utilize estimating the intersection of two direct paths between multiple AIRS. The differences between the two are notable. The former is a complex algorithm that accurately estimates points of intersection through multiple constraints from two AIRS. The former estimates the positioning by generating and solving parametric equations and systems of linear equations and then computes the weighted average of the points of the equations' estimated solutions (point intersections).

3.1.3 U-UAV^{RIS} in Transmission Strategies

UAV trajectory is an important aspect of any UAV approach. Positioning and alignment make the difference between achieving optimal and subpar optimization goals. A hybrid offline–online U-UAV^{RIS} approach that improves overall system performance by leveraging instantaneous and statistical channel state information under Rician fading conditions is seen in [66]. Here, offline conditions refer to the state where U-UAV ground-channel states are very random and dynamic, and data loss rates are higher due to lack of adaptability [66], and the online conditions are the converse of the offline conditions. The authors jointly optimize the maximum achievable rate through the RIS phase shift and U-UAV trajectory based on the statistical channel state information for the offline phase [66]. In the approach's online phase, the U-UAV transmit beamforming and UE scheduling is altered based on the immediate channel state information. Details on the system and channel models and U-UAV trajectory designs are seen in [66]. The authors solve the optimization problem by utilizing stochastic successive convex approximation techniques. The authors prove through simulations and numerical results that a hybrid approach utilizing U-UAV^{RIS} and an online–offline approach based on variations of channel state information efficiently solves the maximal average achievable rate problem under Rician fading conditions [66].

Transmission strategy, channel estimation, and data transmission are important aspects of optimal communication. One method of determining the optimal channel estimation, transmission strategy, and data transmission is through a frame-by-frame analysis of incoming data to an RIS. The approach in [44] uses multi-task learning, where the optimization problem is modeled as a mixed-integer non-linear program. The program outputs the maximum overall throughput of the system. A terrestrial RIS assists the UAV in optimizing the data transmissions within this model. The channel estimation is processed at the UAV level, and the RIS optimizes the transmission throughput. This division of tasks allows for less processing power at the UAV level due to its low battery life and faster processing at the RIS since channel estimation is complicated. The allocation of RIS elements, phase shifts, and UAV position is optimized through the output of the multi-task learning model. By utilizing a learning model at the RIS level, communication is improved greatly according to the results in the paper and therefore achieves the goal of merging RIS and UAV, enhancing QoS.

3.1.4 U-UAV^{RIS} in Energy Efficiency

Beamforming for energy efficiency (EE) is another advantage of utilizing the technology merger of UAV^{RIS}. In [61], the energy efficiency of utilizing an aerial-RIS-aided network and a BS-mounted UAV for emergencies and disaster relief is increased. The UAVs mounted with BS create downlinks with UE in a dead area. Which UAV-mounted BS to use was optimized through the approach. Idle UAVs were placed in sleep mode to conserve energy. The authors optimize which BS is switched on and used to aid the UE. The optimization problem was solved using a Branch-Reduce-and-Bound (BRnB) algorithm, a monotonic optimization with semi-definite steps. The results show that using an RIS to aid energy efficiency proved effective, as shown in [61].

EE is another attribute improved by using UAV^{RIS}. Air-to-ground wireless powered communication networks aided by U-UAV^{RIS} enhance the energy efficiency within the network [52]. The U-UAV^{RIS} helps the hybrid access points facilitate communications to UE in NLoS areas. RIS receive reflected energy from a U-UAV incoming from hybrid access points, which were limited by their inherent energy [52]. An equivalent convex programming solution is presented where an optimization algorithm jointly optimizes the RIS phase shifts, access points' transmit power, and the charging time ratio. Energy efficiency is enhanced by at least 150% [52].

Low-power IoT devices distributed worldwide are known to have short life spans. These devices are crucial within cyber-physical networks to monitor environments. The authors in [53] propose a U-UAV^{RIS} solution for simultaneous wireless information and power transfer (SWIPT). The authors utilize NOMA and non-linear energy models to jointly optimize the U-UAV trajectory, the U-UAV transmit power allocation, the successive interference cancelation decoding order, the power splitting ratio, and the RIS reflection coefficient for sum-rate maximization [53]. The approach incorporates an alternation optimization algorithm, a suc-

cessive convex approximation, and dynamic programming to optimize the attributes mentioned above [53]. The IoT network consists of an RIS-empowered downlink U-UAV SWIPT network. The RIS coordinates channel acquisition, information, and power transmission for the U-UAV and RIS, where the channel state is known and follows a quasi-static flat-fading model. U-UAVs employ NOMA within the network to moderate data transmission between UE and IoT devices. Each NOMA user incorporates the higher priority successive interference cancelation decoding order. The power-splitting receiver decodes the information and assists in power harvesting within the network. Further details of the approach are found in [53]. The results tested against numerical simulations concluded that the maximum sum rate is significantly enhanced when considering the attributes optimized above; the RIS is crucial for channel acquisition information and power transmission, which the U-UAVs assist in the NOMA network [53].

For IoT-based approaches, energy consumption and resource allocation are important constraints that require appropriate optimization to increase the number of devices used in the shared spectrum within the communication network. It is worth noting that approaches such as distributed UAV^{RIS} networks improve the constraints mentioned above by implementing optimized trajectory and phase-shift solutions, power control for resource allocation, as well SWIPT-based approaches, which enhance the coverage area and wireless energy transmission of UAVs to devices within the network [26, 53].

Wireless power transfer by utilizing U-UAV^{RIS} mentioned in [54] allows improvement in EE by optimizing the U-UAV trajectory and hovering location as the RIS reflection coefficient. The authors in [54] propose a successive convex approximation of a minorization–maximization algorithm. This algorithm optimizes the minimum charged energy ground sensors in calculating reflection coefficients. With the optimization of the reflection coefficients comes the joint optimization of the U-UAV trajectory and hovering location. The approach implemented by the authors ultimately shows that by integrating the RIS into wireless power transfer, the overall energy requirements for the application are reduced considerably [54].

3.1.5 U-UAV^{RIS} in Secrecy and Sum Rates

Security in communications can be improved through a high-performance network, and as such, the dynamic duo finds itself applied in the prevention of wiretapping on a communication channel [63]. The authors present an optimization problem that aims to maximize the average worst-case secrecy rate by optimizing the UAV's trajectory, RIS's passive beamforming, and transmit power of the legitimate transmitters. The results were claimed through a series of tests involving an eavesdropper attempting to access channel state information from legitimate transmitters. An assumption was made that the channel state information from the perspective of the eavesdropper needed to be more accurate. The results showed that using a U-UAV and RIS improved the secrecy rate with a communication channel [63].

Similarly, the authors in [65] maximize the sum rate achieved by ground users by optimizing the UAV trajectory, RIS phase shifts, and sub-channel assignments for the backhaul capacity constraint. The idea is to optimize data transmission efficiency by optimizing the bandwidth and allocation for backhaul links with the constraint in mind. The optimization problem follows a successive convex approximation to optimize the UAV placement. The authors assume LoS links between the BS, UAV, and RIS and the UE experiences Rayleigh Fading. Results in the approach showed that the sum rate achieved by ground users increased linearly when the system used an RIS compared to the lack of an RIS [65].

Another approach regarding optimizing the maximum sum rate is seen in [47], where the authors utilize a U-UAV^{RIS} downlink system where a multiple-antenna BS accommodates a single antenna UE. The authors set up the optimization problem to jointly optimize the beamforming at the BS, the RIS phase shift, and the U-UAV 3D placement through a block coordinate descent iterative algorithm. The motivation behind the approach is to improve the downlink in a complex urban environment [47]. An RIS-mounted-U-UAV is deployed to an NLoS area where UE does not have a direct link to the BS. The optimization algorithm was split into two sub-problems: U-UAV position and beamforming or RIS phase shift are optimized alternatively through a block coordinate descent and iterative algorithm. The authors conclude with the results in [47] that the sum rate is enhanced to a significant degree with U-UAV^{RIS} technology due to mobility and reflection qualities.

The sum rate is also enhanced through deep learning techniques. The system sum rate is maximized for multiple users with a single output with a signal incoming from an aerial RIS. The RIS provides downlink signals from ground BS to UE in NLoS areas. The system sum rate is achieved by optimizing the RIS phase shift matrix and flying trajectory jointly. The optimization is completed by translating the points for processing in a deep reinforcement learning network through a deep deterministic policy gradient algorithm. Noise addition effects are minimized by a mapping function ensuring complete constraint satisfaction to increase action decision accuracy [49]. The approach assumes that ground downlinks between the BS and UE are blocked and unavailable. This approach shows the utility and advantages of free mobility and the inclusions of RIS properties to maximize the sum rate in an NLoS area by creating a makeshift LoS area. While there are still losses, the sum rate is maximized and

optimized. What differentiates this solution from others is the utilization of data processing through the deep reinforcement learning algorithm. According to the authors' results, this algorithm significantly improves the achievable system sum rate [49].

3.1.6 U-UAV^{RIS} and Positioning and Coverage

A hybrid concept of implementing dynamic and fixed U-UAV^{RIS} applications is worth exploring. The approach mentioned in [55] presents a university campus-based approach to implementing dynamic U-UAV–RIS and terrestrial RIS to increase the probability of LoS areas and the coverage in non-LoS areas. The authors utilize a global positioning system, machine learning, and clustering of the technologies to increase robustness and coverage areas within a university campus that faces many obstacles and moving objects. This hybrid approach proves that the technology merger's segue improves communications and the robustness of a network given specific channel constraints [55].

For a more current realistic solution, the authors in [9] provide a means for accurate positioning of U-UAVs with respect to RIS. The goal of the approach mentioned above is to maximize the data transfer rate by jointly optimizing the RIS phase shift and the 3D space of the U-UAV. EE and positioning is the main concern of the authors. Deep Q-network and deep deterministic policy gradient algorithms are utilized through the use of deep reinforcement learning [9]. The machine learning algorithms result in a solution for the U-UAV trajectory and passive beamforming. The phase shift of the RIS is altered with respect to the outcome of the learning algorithms to optimize the alignment of the U-UAV to BS signal reflection angles. Further details on the machine learning algorithms that optimize the abovementioned crucial characteristics are seen in [9]. The proposed solution improved energy efficiency by aligning and positioning the U-UAV accordingly while satisfying the BS data transmission requirements.

U-UAV positioning and alignment depend entirely on the application to solve the problem. Some approaches optimize the positioning for a minimal bit-error rate, and others with respect to the optimal energy efficiency of a system [18]. Other approaches utilized assisted devices for path planning as this deployment aspect is crucial to securing the solution's effectiveness to an approach [18]. Details of such positioning can be seen in the UAV survey in [18].

Maintaining LoS links and increasing coverage areas is done by optimizing the deployment and positioning of a UAV with respect to a BS or RIS. A collection of U-UAV^{RIS} is deployed within high-density areas to complete the task mentioned above [56]. Efficiency and performance are crucial for next-generational networks, specifically for the topic of interest, 5G and mmWave frequencies. The authors in [56] develop a framework for sustaining and maintaining LoS links in high-density areas using RIS-mounted U-UAVs. A consensus-based approach increases the coverage area and QoS for all dynamic UE, while the RIS reflects signals to improve efficiency and communication within the high-density areas. The authors conduct tests on the consensus algorithm-utilized effective navigation framework defining several clusters for simulation within the scope of a dynamically changing environment with LoS and NLoS areas [56]. The simulation results provide evidence that the consensus algorithm follows through with the goal of the approach. Further discussion on technical problems with establishing LoS links has been discovered and discussed in detail in [56].

3.1.7 U-UAV^{RIS} and Outage Probability

Performance analysis and outage probabilities are important aspects associated with these intelligent devices. Stress testing and accounting for unforeseen events such as blockages, misalignment, and disorientation are crucial to understanding how intelligent surfaces perform under these circumstances. The authors in [67] do exactly that. The authors present multiple events completed on Monte-Carlo-based simulations to test for dynamic outage probabilities according to specific events. The authors account for fading conditions, disorientation, misalignment, and hardware faults. Tests are completed on specific sets of U-UAV^{RIS} conditions, and stress tests are completed to compute diversity order and outage probabilities.

3.2 T-UAV^{RIS}

The merger of UAVS and RIS is restricted to U-UAVS and T-UAVS. The main difference between U-UAVs and T-UAVs is that T-UAVs have a direct backhaul link and a lower degree of freedom. The advantage of having a direct backhaul link through a tethered medium allows for many applications. Using a tethered link allows for direct data transmission and consistent power between the tether station and the UAV at the cost of degrees of freedom.

Due to the convenience of constant power provision from a tethered link, a T-UAV can be optimized for usage with an active RIS, which consumes more power than a passive RIS. Details on an active RIS are mentioned in the Background section. Utilizing the tethered link and the active RIS helps amplify the incident angle based on a specific location constrained by the T-UAV. This claim shows that using a T-UAV with a constant tethered powered link makes an active RIS more effective for longer deployment applications. For specificity, large-scale path loss, small-scale fading, and mmWave beamforming modeling are discussed. There exist minimal precedents on T-UAV^{RIS}, but notable applications are mentioned below.

3.2.1 T-UAV^{RIS} in High-Throughput Communication

Using a T-UAV comes with many advantages. Reference [16] describes some of the advantages and use cases of applying T-UAVs in practice. The advantages of utilizing T-UAVs are the power consumption and life of the devices. The power consumption is heavily decreased since some processing power is handled at the linking station. The cost of this implementation is considerably less than a U-UAV due to the lack of reason for optimizing the location of the T-UAV midflight. This reason allows for deploying T-UAVs within smaller rural areas to increase and strengthen signal communication. The link from the station is not prone to interruption. The existence of the link allows for higher data traffic which means there is a higher capacity through the tether link.

In the case of T-UAV^{RIS} for backhauling, if there is power within the system model of interest for a specific problem, then the concept of backhauling is negligible; as such, this emphasizes that RIS can be used to improve communication hand-in-hand with a T-UAV. One application that utilized the power of the tethered link is seen in [69] where a framework called CURE where radiofrequency energy harvesting (RFEH) is merged with a massive cell-free MIMO (CFmMIMO), T-UAV, and RIS network to enhance the wireless power transfer to Internet-of-Things (IoT) devices. The problem addressed in this approach is enhancing the RFEH through an RIS-assisted network where the cell-free access points are mounted on T-UAVs over the coverage area. The wireless power transfer from the T-UAV is then reflected off the RIS with the metasurface's manipulative nature to optimize the phase angle shift and maximize the signal transmitted to an IoT device. The authors tested their approach on a max-min fairness algorithm, which resulted in higher energy transfer and data transmission.

3.2.2 T-UAV^{RIS} in Signal Pathways

The disadvantage of using a tethered link is the limited degree of freedom provided compared to a U-UAV. These devices hover within a hemispheric area at specific positions at given heights, a certain distance from the link station. This region is the hovering region, which is limited compared to a U-UAV. The approach mentioned in [16] suggests increasing the number of hovering regions for T-UAV and linking stations within given areas where the links are optimized for maximum signal optimization. A suggestion for the approach mentioned earlier is to utilize terrestrial RIS to enhance and optimize signal paths within rural areas or congested areas, reducing the need to mitigate the hemispheric area using altitude. Another suggestion is utilizing T-UAV-mounted RIS for signal reflection and a T-UAV as utilized in the above approach. This suggestion allows for stronger power utilization in an RIS and UAV and higher processing power at the RIS level.

3.2.3 T-UAV^{RIS} in Energy Efficiency

Due to the consistent power advantage in T-UAV, EE can be enhanced following the solution proposed. A measure of EE can be determined and derived from the average bit-error rate within a communication environment. Discussed in [35] is a T-UAV RIS approach where the RIS supports single, full-angle reflection and is assisted by a T-UAV. The aerial RIS can reflect intelligently and improve ground node LoS communication, strengthening the overall channel. The channel is assumed to have dual-hop communication, and the channel state information is known to ensure maximizing the SNR. The results were derived against the average bit error rate based on modulation order on many passive RIS elements. The results showed that with more passive elements, the average bit error rate degraded and improved EE while providing a reliable environmental communication channel.

3.3 Channel Models

Channel estimation and modeling are two main challenges of any UAV^{RIS} approach [22]. Considering dynamic environments, obstacles, fading, and physics-based models are not easy. A suitable channel model is required to conduct experiments and set up suitable system models. The results of an approach can greatly differ if a channel model needs to be set up properly. Each respective approach mentioned above follows its channel and system model and provides details on channel estimation. This section provides examples of channel models that are used and worth noting, as well as the guidelines supporting the channel models used in the respective approaches.

3.3.1 Resource Allocation and Placement

An interesting choice for channel models is seen in this approach [65]. The communication links are assumed to have Rayleigh fading considerations from blockages, and links are LoS propagated. Following the approach in [68], the authors of [65] assume the received signal at the k^{th} ground unit is denoted as $y_k = \sqrt{p}((\mathbf{h}_k^{\text{RIS-Tx}})^H \Phi \mathbf{h}^{\text{UAV–RIS}} + h_k^{\text{UAV-Tx}} + n^{\text{G}}$ and p is the transmit power of the U-UAV for ground unit k on each sub-channel, n^{G} expresses the respective ground unit's additive white Gaussian noise, and mean ($\mu = 0$), and variance (σ^2) [65]. The channel coefficients link between the U-UAV and ground unit k, U-UAV^{RIS}, and RIS to ground unit k are $h_k^{\text{UAV-Tx}}$, $\mathbf{h}^{\text{UAV-RIS}}$, and $\mathbf{h}_k^{\text{IG}}$ [65]. Φ is the RIS phase shift matrix, and the RIS consists of $I_r \times I_c$ passive reflection elements. The expressions for the channel coefficient links are:

$$h_k^{\text{UAV-Tx}} = \sqrt{\frac{\beta_0}{(d_k^{\text{UAV-Tx}})^2}}, \qquad \forall k, \tag{1}$$

$$\mathbf{h}^{\text{UAV-RIS}} = \sqrt{\frac{\beta_0}{(d^{\text{UAV-RIS}})^2}}[1, e^{-j\frac{2\pi d}{\lambda}V_i}, ..., e^{-j\frac{2\pi d}{\lambda}(I_r\text{-}1)V_i}]^H \otimes [1, e^{-j\frac{2\pi d}{\lambda}V_j}, ..., e^{-j\frac{2\pi d}{\lambda}(I_r\text{-}1)V_j}]^H \quad (2)$$

$$\mathbf{h}_k^{\text{RIS-Tx}} = \sqrt{\frac{\beta_0}{(d_k^{\text{RIS-Tx}})^2}}[1, e^{-j\frac{2\pi d}{\lambda}V_l}, ..., e^{-j\frac{2\pi d}{\lambda}(I_c\text{-}1)V_l}]^H \otimes [1, e^{-j\frac{2\pi d}{\lambda}V_n}, ..., e^{-j\frac{2\pi d}{\lambda}(I_c\text{-}1)V_n}]^H \alpha^{\text{RIS-Tx}}, \forall k, \quad (3)$$

where the coeffiecients V_x are represented as $V_i = \sin\theta^{\text{UAV-RIS}}\cos\xi^{\text{UAV-RIS}}$, $V_j = \sin\theta^{\text{UAV-RIS}}\sin\xi^{\text{UAV-RIS}}$, $V_l = \sin\theta_k^{\text{RIS-Tx}}\cos\xi_k^{\text{RIS-Tx}}$, $V_n = \sin\theta_k^{\text{RIS-Tx}}\sin\xi_k^{\text{RIS-Tx}}$. β_0 is the channel gain at a reference distance of 1 m, k is the path loss exponent, and λ is the carrier wave wavelength [65]. The random scattering components are $\alpha^{\text{RIS-Tx}}$. $(\theta^{\text{UAV-RIS}}, \xi^{\text{UAV-RIS}})$, $(\theta^{\text{RIS-Tx}_k}, \xi^{\text{RIS-Tx}_k})$, are the vertical and horizontal angle-of-departures from the U-UAV to the RIS and from the RIS to ground unit k, and H is the U-UAV altitude [65].

3.3.2 3D Trajectory and Phase Shift

The optimal trajectory of a UAV is crucial in any UAV approach. This parameter is similar to the UAV placement parameter. Merging the advantages of RIS phase shift, the optimal trajectory and phase shift can be used hand-in-hand to achieve maximum energy efficiency, data rate, and throughput while decreasing the overall propulsion energy of the U-UAV. The system model assumes that the UAV follows a predefined flight path and is equipped with a directional antenna that can be pointed toward the RIS. The RIS consists of N reflecting elements that can be adjusted to achieve a desired phase shift. The communication between the U-UAV and the RIS is modeled using a narrowband channel with a flat fading coefficient [58]. The communication environment is then optimized while considering the location of ground UE.

The scheme presented in [58] configures a system consisting of a U-UAV equipped with a transmitter and an RIS consisting of multiple reflecting elements. The proposed approach uses deep reinforcement learning, where the system learns through trial and error to maximize the reward function, defined as the communication rate between the UAV and the ground station, to optimize the trajectory and phase shift. The reward function considers the UAV's trajectory, the phase shift of the RIS elements, and the channel characteristics [58].

The channel gain model from the [58] was replicated and used where

$$g_n^{\text{U-UAV-RIS}} = \frac{\xi}{d_n^{\text{U-UAV-RIS}}}[1, e^{-j\frac{2\pi}{\lambda}d_{\text{RIS}}\phi_k^{\text{U-UAV-RIS}}\psi_k^{\text{U-UAV-RIS}}}, ..., e^{-j\frac{2\pi}{\lambda}(M_{\text{RIS}}-1)d_{\text{RIS}}\phi_k^{\text{U-UAV-RIS}}\psi_k^{\text{U-UAV-RIS}}}]^T \otimes [1, e^{-j\frac{2\pi}{\lambda}d_c\varphi_k^{\text{RIS-UE}}\psi_k^{\text{RIS-UE}}}, ..., e^{-j\frac{2\pi}{\lambda}(M_c-1)d_{\text{RIS}}\varphi_k^{\text{RIS-UE}}\psi_k^{\text{U-UAV-RIS}}}]^T \quad (4)$$

is the channel gain of the UAV$^{\text{RIS}}$ such that n represents the time slot, λ is the carrier wavelength, ξ is the path loss at the reference distance of 1 m, $d_n^{\text{U-UAV-RIS}} = \sqrt{(H_n^{UAV} - z_{RIS})^2 + (L_n^{UAV} - w_{RIS})^2}$, H_n^{UAV} is the height of the U-UAV at the nth time slot, $w_{RIS} = [x_{RIS}, y_{RIS}]^T$ and z_{RIS} are the horizontal and vertical dimension of the location of the first RIS element, L_n^{UAV} is the approximate trajectory of the U-UAV at the nth time slot, $\phi_k^{\text{U-UAV-RIS}} = \frac{x_k - x_{RIS}}{d_k^{\text{RIS-UE}}}$ and $\varphi_k^{\text{RIS-UE}} == \frac{y_k - y_{RIS}}{d_n^{\text{RIS-UE}}}$ are the cosine and sine of the horizontal angle-of-departure to the kth UE, and $\psi_k^{\text{RIS-UE}} = \frac{z_{RIS}}{d_k^{\text{RIS-UE}}}$ is the sine of the vertical angle-of-departure of the signal to the kth UE [58].

3.3.3 RF Links and LoS Modeling

A channel model is also required for T-UAV$^{\text{RIS}}$ approaches. The authors in [70] discuss multiple channel models and channel estimation techniques for various approaches regarding networked tethered flying platforms. Low-altitude platform channel models within the tethered scheme are considered for the scope of this survey.

Radiofrequency links are considered for large-scale and small-scale fading. For the case of large-scale path loss, the distribution of the buildings is modeled following a Rayleigh distribution such that $f(H_t) = \frac{H_t}{2\gamma^2}\exp(\frac{Ht^2}{2\gamma^2})$ where H_t is the buildings' height in meters. Thus, the LoS probability is modeled as the following:

$$\text{P(LoS)} = \prod_{n=0}^{m}[1 - \exp(-\frac{[ht_{Tx} - \frac{-(n+\frac{1}{2})(ht_{Tx} - ht_{Rx})}{m+1}]^2}{2\gamma^2})], \quad (5)$$

where ht_{Tx} and ht_{Rx} are the heights of the transmitter and receiver. $m = \text{floor}(r\sqrt{p_\alpha p_\beta - 1})$ where r is the ground projection of the distance between the Tx and Rx [70]. The LoS probability includes these parameters p_α, which is the ratio of built-up land area to the total land area, p_β is the number of buildings per km^2, and p_γ is the buildings' heights' scale parameter [70]. The probability of LoS can be expressed as a function of θ, the elevation angle, which is the angle between the slant range and the horizon plane, such that

$$\text{P(LoS}, \theta) = \frac{1}{1 + a_1\exp(-b_1(\theta - a_1))}, \quad (6)$$

where a_1, b_1 are functions of p_α, p_β, and p_γ [70]. The probability of NLoS is P(NLoS) $= 1 -$ P(LoS) [70]. The path loss is then modeled as:

$$\begin{aligned} &\mathrm{PL}(\alpha_{\mathrm{PL}}, \theta, d_{\text{Tx-Rx}}) = d^{-\alpha_{\mathrm{PL}}(\theta)} \\ &\times [\mathrm{Loss}_{\mathrm{LoS}} \cdot \mathrm{P}(\mathrm{LoS}, \theta) + \mathrm{Loss}_{\mathrm{NLoS}} \cdot \mathrm{P}(\mathrm{NLoS}, \theta)], \end{aligned} \tag{7}$$

where $d_{\text{Tx-Rx}}$ is the distance between Tx and Rx, $\mathrm{Loss}_{\mathrm{LoS}}$ and $\mathrm{Loss}_{\mathrm{NLoS}}$ are the mean additional losses for the LoS and NLoS transmissions, and α_{PL} is the path loss exponent [70]. The path loss exponent is expressed as:

$$\begin{aligned} &\alpha_{\mathrm{PL}} = a_2 \mathrm{P}(\mathrm{LoS}, \theta) + b_2 \\ &a_2 = \frac{\alpha_{\frac{\pi}{2}} - \alpha_0}{\mathrm{P}(\mathrm{LoS}, \frac{\pi}{2}) - \mathrm{P}(\mathrm{LoS}, 0)} \cong, \alpha_{\frac{\pi}{2}} - \alpha_0 \\ &b_2 = a_0 - a_2 \mathrm{P}(\mathrm{LoS}, \theta) \cong a_0, \end{aligned} \tag{8}$$

where $\alpha_{\frac{\pi}{2}}$ and α_0 are path loss exponent values at $\theta = \frac{\pi}{2}$ and $\theta = 0$, respectively, and further details on the channel model for large-scale fading are seen in [70].

Rayleigh, Rician, Nakagami-m, and Loo fading models are referenced for small-scale fading along with a generalized extended distribution encompassing many distributions for radio frequency links, including mmWave frequencies. Derivations of the fading models are further discussed in [70]. The distribution used is called an extended generalized-$\mathcal{K}$ where the PDF is expressed as:

$$\begin{aligned} &f_y(y) = \frac{2\psi}{\Gamma(m_s)\Gamma(m)} \left(\frac{\mathcal{B}_s \mathcal{B}}{\Omega}\right)^{m\psi} y^{2m\psi - 1} \\ &\times \Gamma\left(m_s - m\frac{\psi}{\psi_s}, 0, \left(\frac{\mathcal{B}_s \mathcal{B}}{\Omega}\right)^{m\psi} y^{2\psi}, \frac{\psi}{s}\right), \end{aligned} \tag{9}$$

where Ω is the average power of the received signal envelope, m and m_s are the fading severity and shadowing severity, respectively, ψ and ψ_s are the fading shaping and shadowing shaping factors, respectively, and $\mathcal{B}_s$ and $\mathcal{B}$ are functions defined in [70] as

$$\begin{aligned} \mathcal{B}_s &= \frac{\Gamma\left(m_s + \frac{1}{\psi_m}\right)}{\Gamma(m_s)} \\ \mathcal{B} &= \frac{\Gamma\left(m + \frac{1}{\psi_m}\right)}{\Gamma(m)}. \end{aligned} \tag{10}$$

High-gain directional beams are required to compensate for high path loss and scattering in mmWave frequencies for beamforming. The authors in [70] approximate the directional gain through a simple sectored antenna model where the gain ($G(\Psi)$) is $G_{\max}$ if the azimuth angle (Ψ) is within the half-power beamwidth or $G_{\min}$ otherwise. Though unlikely, when available, perfect beam alignment assigns an effective antenna gain of $G_{\mathrm{eq}} = G_{\max}^2$ [70]. A more realistic approach includes beam steering errors (ϵ) which follow a Gaussian distribution with $\mu = 0$ and variance σ_e^2; since the gain angle is symmetric, the beam steering error, $|\epsilon|$, is considered. This consideration implies that $|\epsilon|$ follows a half-normal distribution with CDF $F_{|\epsilon|}(x) = \mathrm{erf}(x/\sqrt{2\sigma_e})$, and the PDF of the effective antenna gain is:

$$\begin{aligned} &f_{G_{\mathrm{eq}}}(x) = F_{|\epsilon|}\left(\frac{\Phi}{2}\right)^2 \delta_{x - G_{\max}} \\ &+ 2F_{|\epsilon|}\left(\frac{\Phi}{2}\right)\left(1 - F_{|\epsilon|}\left(\frac{\Phi}{2}\right)\right)\delta_{x - G_{\max}G_{\min}} \\ &+ \left(1 - F_{|\epsilon|}\left(\frac{\Phi}{2}\right)\right)^2 \delta_{x - G_{\min}} \end{aligned} \tag{11}$$

where $\delta_{(\cdot)}$ is the Kronecker delta function [70]. The models mentioned above show good examples of channel models with the appropriate fading conditions for tethered schema, and further details are seen in [70].

3.3.4 Challenges and Modeling

A valid concern regarding a channel model is its linearity and the physics involved with the application. For example, the channel models in [71] are sufficient for free-space applications. Channel models and results are inaccurate if physics-based constraints such as scattering RIS, multiplicative fading, and mesoscopic correlations are not considered.

In nonlinear, non-free-space models, scattering and other physical constraints are considered. The authors in [72] present two cases to describe the rich scattering of RIS. The first case mentioned analyzes multipath channel impulse response, and the second case analyzes an RIS-tunable environment that localizes non-cooperative UE by leveraging through analog multiplexing [72]. Due to the different conditions of EM wave propagation, scattering models require reconsideration. Fine-grained control of the EM field used in the approach improves beamforming accuracy. Another design consideration is that incoming signals in the direction of the RIS are sourced from all possible directions as opposed to one single direction. The common expression of incident and phase coefficients as meta-atoms can be discarded due to the number of directions associated with incoming signals. The authors of [72] suggest utilizing the results of the case studies in their paper as a means to implement RIS in various ways within rich scattering environments. Examples of those means are using an RIS as a localization accuracy enhancer and a processor for EM wave propagation.

An example of an approach that utilizes the above guidelines is in [73], where the RIS dynamically estimates the perturbers' status based on an auxiliary wireless channel. The results are demonstrated on a physics-based fading model

of RIS-parameterized communication. The idea of [73] is to dynamically parameterize a perturber's RIS configuration and status within a given time window to alter and adapt to rich scattering conditions while cohering with physics models of non-free space communication and channel environments. The channel model follows an application of the Beaulieu–Xie fading model, which is widely known to be an accurate and compelling reference for modeling realistic environments [64, 73–75].

More details on the implementation, derivations, and applications of the models mentioned above are seen in [74, 75].

In [64], the authors conduct performance analysis for a decode-and-forward wireless system aided by a U-UAV^{RIS}. The U-UAV within the urban environment follows the 3-dimensional waypoint model at low altitudes where a relay station propagates the U-UAV's signal to terrestrial RIS to a BS [64]. The dynamic, terrain-dependent UAV-to-RIS channel model follows the Beaulieu–Xie fading model as mentioned in [74, 75], and the relay station-to-RIS and RIS-to-BS follow a rice fading model due to the LoS link available [64]. The performance analyses express the outage probability, average bit error rate, and ergodic channel capacity [64]. Details of the numerical results can be seen in [64] as system performance is concluded to improve with respect to the increase of some crucial parameters.

4 Case Studies

4.1 Case Study 1: Fronthaul Outage Compensation

4.1.1 Motivation

Existing work focuses on terrestrial RIS due to the benefits of integrating RISs into the cellular environment, such as low cost, energy-efficient, and spectrum efficiency, which are deployed on the facades of the buildings, which still have drawbacks, such as the willingness of owners of the buildings to rent the facades which may also block the building windows' view. In addition, mounting RIS panels on the buildings' facades will limit the proper operation to the scenario where the source and destination are on the same side, i.e., on the same half-sphere in front of the building. On the other hand, mounting the RIS panel on an untethered UAV (U-UAV) will increase the probability of achieving LoS connectivity in addition to allowing 360° panoramic full-angle reflection [42]. Moreover, the U-UAV can adjust the RIS location periodically, according to the user movement, thus maintaining persistent LOS links with both source and destination. However, the U-UAV service time will be limited to its battery capacity (the flying time will be limited to tens of minutes).

These attributes motivated us to present our U-UAV^{RIS} and T-UAV^{RIS} approach where we consider colocating a U-UAV^{RIS} or a T-UAV^{RIS} to selected small gNBs (SgNBs) in 5G and beyond networks. Given that most SgNBs are fronthauled using wireless links, there is a relatively high probability that any links can fail. Once a fronthaul failure occurs, the T-UAV^{RIS}, colocated with the SgNB, will fly vertically to a pre-defined altitude (or a U-UAV^{RIS} which can fly vertically and horizontally) to achieve one or more LoS alternate fronthaul links. If the fronthaul failure occurs to one of the SgNBs that is not equipped with a UAV^{RIS}, a neighboring UAV^{RIS} equipped SgNB will launch its UAV^{RIS} to heal the failed SgNB. This fail-safe reflects the importance of the pre-planning phase, where the main objective is to minimize the number of colocated UAV^{RIS} subject to a guaranteed minimum fronthaul achievable rate in case of the failure of any fronthaul link of any SgNB.

4.1.2 UAV^{RIS} Fronthaul Outage Compensation Scheme

We consider a dense network for our fronthaul outage compensation scheme where SgNBs are distributed either at the street level or above buildings in the presence of different-shaped buildings. We consider three different types of SgNBs:

1. Failed SgNB (FSgNB): is a SgNB that is suffering from fronthaul failure, and the proposed scheme is mitigating this failure by using UAV^{RIS}
2. Donor SgNB (DSgNB): is the SgNB that provides the fronthaul connection to the FSgNB before the occurrence of the failure
3. Neighboring SgNB: this is a neighboring SgNB to the FSgNB that is going to provide the alternate fronthaul link via UAV^{RIS}. For simplicity, we did not show DSgNB in Fig. 6.

As shown in Fig. 6, the FSgNB is not equipped with our proposed solution, i.e., UAV^{RIS}; however, the NSgNB is equipped and launched its UAV^{RIS} to initiate the healing process. Note that the distance between NSgNB and FSgNB is d.

We introduce two types of UAVs, T-UAV^{RIS} and U-UAV^{RIS}, to show how the orientation of the UAV on the x-axis will affect the achievable fronthaul rate of the FSgNB. Both UAVs are placed at an altitude of h, and the U-UAV can move anywhere on the x-axis between NSgNB ($x = 0$) and FSgNB ($x = d$). Given the building that is blocking the LoS communications between FSgNB and NSgNB, both UAVs can achieve connectivity via two LoS links aided by either the T-UAV^{RIS} or the U-UAV^{RIS}.

Compared to the RIS mounted on the facades of buildings, T-UAV^{RIS} has multiple appealing advantages. First, with an

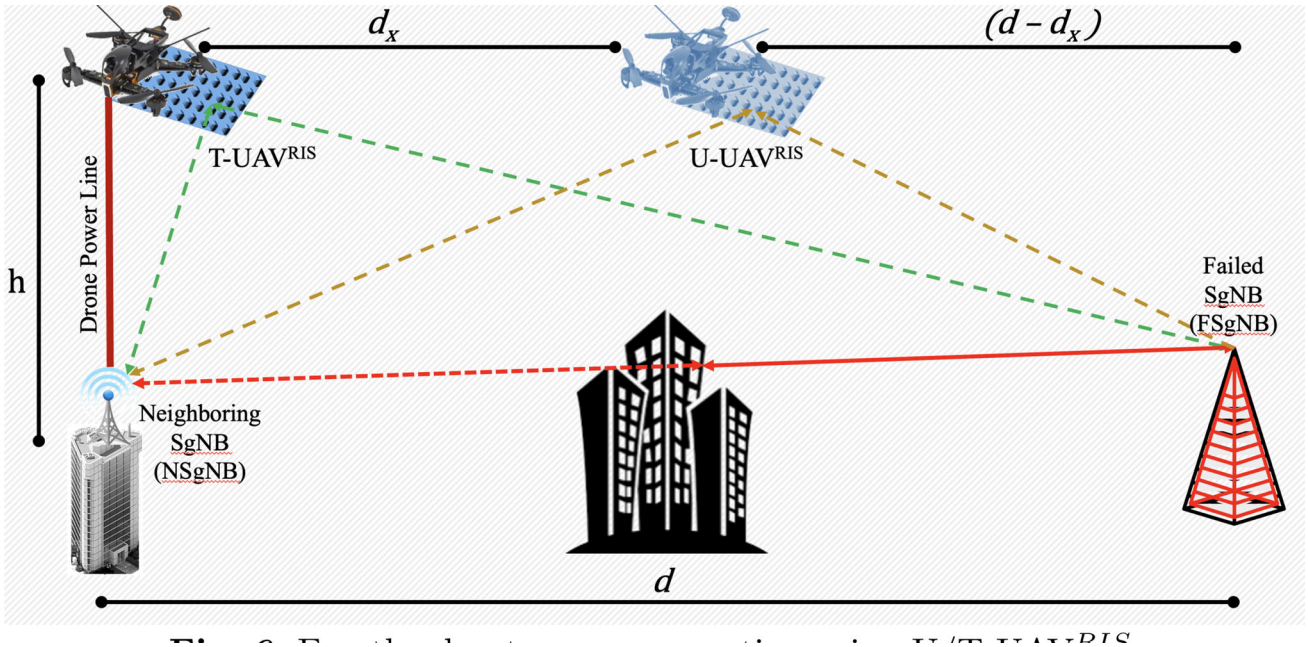

Fig. 6 Fronthaul outage compensation using U/T-UAV^{RIS}

elevated position, T-UAV^{RIS} can establish LoS links between FSgNB and NSgNB with high probability, which leads to a higher fronthaul rate compared to the terrestrial RIS, thereby offering a new degree of freedom to enhance the degree of recovery from failure. Second, equipping one SgNB with T-UAV^{RIS} can heal its fronthaul failure and neighboring SgNB fronthaul failures.

Despite the appealing advantages of the proposed approach, it is still susceptible to some limitations:

- The maximum altitude that the T-UAV^{RIS} can reach is limited to the city/state/federal regulations, which may limit its functionality of achieving a clear LoS between the source and the destination. Also, the optimal tethering location may not be available with some restrictions (for example, privacy) related to flying UAVs near buildings.
- The tethering property will limit the inclination angle of the T-UAV^{RIS}, which limits the mobility of the T-UAV^{RIS} to a few meters around the SgNB, given that the U-UAV^{RIS} will mainly suffer from the depletion of its battery.

4.1.3 Simulation Results

The numerical results simulated using MATLAB are demonstrated in this section to showcase the effectiveness of our proposed approach and explore the advantages of implementing RIS to alleviate X-haul failures in 5G networks. To further investigate details of this simulation's code, refer to [76] where an example of RIS is shown compared to Decode-and-Forward Relaying.

We consider two SgNBs, a U-UAV^{RIS} with N reflecting elements. The locations of the SgNBs and the UAVs are shown in Fig. 6. Denote the horizontal distance between the FSgNB and NSgNB by d (100 ms in our simulation setup), the distance between the U-UAV^{RIS} and NSgNB as d_x, the distance between the U-UAV^{RIS} and FSgNB as $d - d_x$, the altitude of the U-UAV^{RIS} as h. It is assumed that LoS links dominate the NSgNB–IRS and IRS–FSgNB channels, an LoS link dominates the DSgNB–FSgNB channel, and an NLoS link dominates the NSgNB–FSgNB channel.

In this setup, we configure the transmit power to be 17 dBm, the altitude of the U-UAV^{RIS} to be 15 m and 35 m based on the two presented scenarios, the minimum threshold for the fronthaul rate to be 1.5 bits/s/Hz, and the distance between NSgNB and FSgNB is d = 100 m. We used three values for the number of RIS elements: 75, 200, and 500. It is worth noticing that as the number of elements increases, the RIS panel's weight will increase, and the power needed for these elements to operate will increase. In addition, the smart controller's power consumption will increase. All these drawbacks of increasing the number of reflecting elements will not affect our proposed model, given that the tethering property provides a continuous power source.

We modeled the channel gains for the sub-6 GHz (3 GHz) using the 3GPP Urban Micro [77]. We used both the LoS and NLoS models. Our analysis considers the channel deterministic, as the RIS elements reflect passively with a fixed phase shift and do not have any signal processing capabilities. The

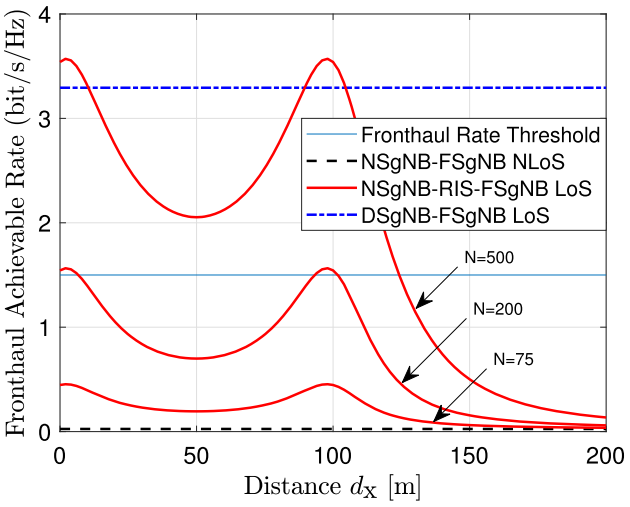

Fig. 7 Fronthaul achievable rate versus distance ($h = 15$ m)

destination, i.e., FSgNB, is supposed to know the channel, and the phase shift can be optimized. This assumption is made due to the non-trivial nature of channel estimation for RIS. However, recent studies such as [78] have presented a general framework for estimating the channel. Additionally, authors in [79] proposed incorporating non-uniformly distributed active elements into the RIS panel to facilitate channel training/estimation through deep learning techniques.

The fronthaul achievable rate in Figs. 7 and 8 can be calculated using the following three equations:

$$R_{\mathrm{DF}}^{\mathrm{LoS}} = \log_2\left(1 + \frac{p\beta_{\mathrm{DF}}^{\mathrm{LoS}}}{\sigma^2}\right) \tag{12}$$

$$R_{\mathrm{NF}}^{\mathrm{NLoS}} = \log_2\left(1 + \frac{p\beta_{\mathrm{NF}}^{\mathrm{NLoS}}}{\sigma^2}\right) \tag{13}$$

$$R_{\mathrm{NIF}} = \log_2\left(1 + \frac{p\left(\sqrt{\beta_{\mathrm{NF}}^{\mathrm{NLoS}}} + \epsilon\, N_x \sqrt{\beta_{\mathrm{NIF}}^{\mathrm{LoS}}}\right)^2}{\sigma^2}\right) \tag{14}$$

where $R_{\mathrm{DF}}^{\mathrm{LoS}}$ is the achievable rate of the LoS link between DSgNB and FSgNB, $R_{\mathrm{NF}}^{\mathrm{NLoS}}$ is the achievable rate of the NLoS link between the NSgNB and FSgNB, R_{NIF} is the virtual LoS link from the NSgNB to the RIS then from the RIS to the FSgNB, p is the transmitted power, $\sqrt{\beta}$ is the deterministic flat-fading channel gain, and N is the number of reflecting elements in the RIS panel. We are interchangeably using the terms channel capacity and achievable rate, given that the achievable rate unit is bit/s/Hz.

As shown in Fig. 7 where the altitude of the U-UAV$^{\mathrm{RIS}}$ is set to be 15 m, the fronthaul achievable rate before the occurrence of failure, i.e., DSgNB–FSgNB LoS curve, is around 3.25 bits/s/Hz. Once the failure occurs and before the launching of the U-UAV$^{\mathrm{RIS}}$, the NLoS fronthaul link between the NSgNB and the FSgNB, i.e., NSgNB–FSgNB NLoS curve, is very close to 0 bits/s/Hz which shows that without using our proposed solution, the FSgNB will not achieve the minimum required threshold rate. Finally, the three curves bounded by the DSgNB–FSgNB LoS curve and NSgNB–FSgNB NLoS curve represent the fronthaul achievable rate when launching the U-UAV$^{\mathrm{RIS}}$ and moving it from $x = 0$ m, i.e., NSgNB location, passing over the FSgNB at $x = 100$ m and continuing until reaching $x = 200$ m. For the three curves that represent different numbers of reflecting elements, it is observed that there are two peaks at $x = 0$ m and $x = 100$ m where the NSgNB and FSgNB are located, respectively. This shows that the optimal location for U-UAV is to hover above either the NSgNB or the FSgNB. Also, for $N = 200$, we can achieve the fronthaul threshold rate at these two locations only. More specifically, when $N = 500$, the fronthaul achievable rate exceeds that of the LoS rate at $x = 0$ m and $x = 100$ m. This occurs under the condition that all reflecting elements are dedicated to reflecting the received signal from the NSgNB to the FSgNB.

To achieve the fronthaul rate threshold and based on the intersection of the fronthaul achievable rate threshold horizontal line and the RIS curves, we have to equip the U-UAV$^{\mathrm{RIS}}$ with reflecting elements ranging from 200 to 500 and locate the U-UAV$^{\mathrm{RIS}}$ vertically above either the NSgNB, i.e., $x = 0$ m or the FSgNB, i.e., $x = 100$ m. This is the main motive behind proposing our T-UAV$^{\mathrm{RIS}}$, where the UAV should be tethered to one of the SgNBs.

It is worth noting that as the U-UAV$^{\mathrm{RIS}}$ moves away from the two SgNBs, i.e., $d > 100$ m, the achievable rate degrades rapidly until reaching the NSgNB–FSgNB NLoS rate.

For the same simulation setup and the same parameters except increasing the altitude of the U-UAV$^{\mathrm{RIS}}$, h, from 15 to 35 m, Fig. 8 shows that increasing the altitude of the UAV degraded the fronthaul achievable rate by more than 50% where even with $N = 500$ reflecting elements, our proposed approach can achieve the fronthaul rate threshold only at the two previously proposed locations. To achieve a better fronthaul rate, the source or the destination has to increase the transmit power, or the UAV has to fly at a lower altitude. Moreover, for $N = 200$ and 75 reflecting elements, we lost the advantage of having the UAV tethered to the NSgNB or the FSgNB, where any point on the x-axis will give approximately the same fronthaul achievable rate.

4.2 Case Study 2: 3D Trajectory and Phase Shift

4.2.1 Motivation

For the second case study, a U-UAV$^{\mathrm{RIS}}$ system is analyzed for 3D trajectory and phase shift designs. The case study is based on the work in [58] described in Sect. 3.3.2. The motivation

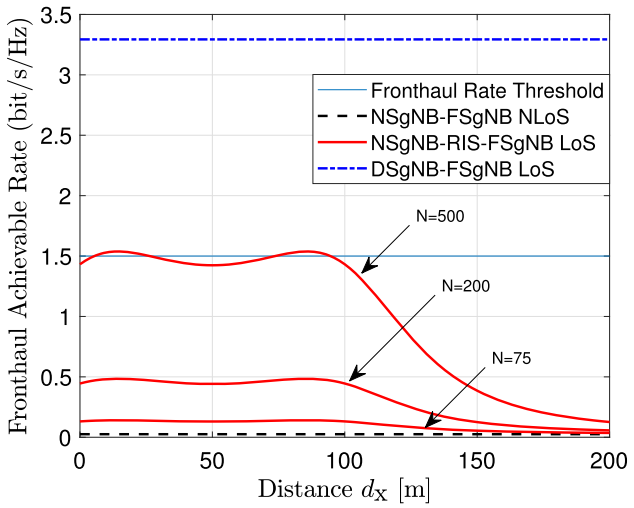

Fig. 8 Fronthaul achievable rate versus distance ($h = 35$ m)

involves assessing and improving the performance of a U-UAV$^{\text{RIS}}$ communication system consisting of a UAV and an RIS, which is mounted on the facade of a building while the users are distributed all around the serving area. The authors propose a novel approach that optimizes both the 3D trajectory of the U-UAV and the phase shift of the RIS elements to maximize the system's communication rate and minimize the U-UAV propulsion energy. This work addresses the challenges associated with RIS-assisted UAV communication systems, such as maintaining an optimal UAV trajectory while optimizing the RIS elements' phase shift. The proposed approach aims to overcome these challenges by leveraging deep reinforcement learning to optimize the trajectory and phase shift in a coordinated and adaptive manner [58]. The study aims to provide a more efficient and effective solution for RIS-assisted UAV communication systems, which could have important applications in remote sensing, surveillance, and search and rescue operations where reliable communication rates and stable UAV trajectories are critical for the mission's success, by optimizing the trajectory and phase shift in a coordinated and adaptive manner using deep reinforcement learning [58].

4.2.2 3D Trajectory and Phase Shift Scheme

For the case study, the number of RIS elements is static, and the height of the UAV's trajectory is set to vary to determine how communication is improved within the environment by analyzing the data rate and energy efficiency. The system's goal is to maximize the communication rate between the UAV and a ground station by optimizing the 3D trajectory of the UAV and the phase shift of the RIS elements. To limit the scope of the case study and provide the necessary information, the minimum trajectory height of the U-UAV is adjusted to compare the cumulative distribution function of the data rate and the energy efficiency when considering an approach without RIS assistance, with RIS assistance but without optimal phase shift, and with RIS assistance and optimal phase shift.

With this approach's advantages (increasing the probability of line of sight and minimizing the U-UAV power consumption) come the inevitable disadvantages of any UAV-based approach, which are:

- Regulatory approvals: Depending on the country and the intended use of the UAV, regulatory approvals may be required for flying the UAV beyond the visual line of sight and for using RIS technology. In addition, the UAV operator may need special permits to operate in restricted airspace, near airports, or in populated areas.
- Interference: RIS technology uses electromagnetic waves to modify the propagation of radio frequency signals, which can potentially interfere with other wireless systems and devices. Using RIS technology on UAVs may require additional regulatory approvals and testing to ensure that it does not interfere with other wireless systems, such as GPS, radar, or civil aviation systems.
- Durability limitations: RIS technology may be vulnerable to damage from environmental factors, such as weather conditions, which could impact its ability to function properly and safely during UAV flight.

4.2.3 Simulation Results

This section presents the numerical results generated using Python to analyze the proposed scheme's effectiveness with regard to adjusting the 3D trajectory of the U-UAV and investigate the data rate in kbps and propulsion energy in KJ. To further investigate details of this simulation's code, refer to [58, 80].

The proposed scheme, as seen in Fig. 9, considers an aerial U-UAV with minimum height, $h_{\min}$, and maximum height, $h_{\max}$. The proposed scheme aims to analyze the effectiveness of the phase shift and 3D trajectory of the U-UAV with a broad range of hovering heights. The U-UAV was assigned $h_{\min} = 15$ m and $h_{\max} = 100$ m. The RIS consists of $M_c \times M_r$=100×100 reconfigurable elements where the phase shift is optimized with respect to the UE locations where there are $k = 4$ UEs. The channel model used is based on [58] as described in Sect. 3.3.2.

The UE locations were scattered diagonally across a 3D grid. The four instances of UE exist in the 3D grid of the assumed environment at (x, y, z) coordinates of (400,400,0), (780,780,0), and (1250,1250,0), respectively. The locations were chosen to understand the behavior of the scheme when the user is close to the reference origin, in the middle of the environment, and on the opposite diagonal from the reference

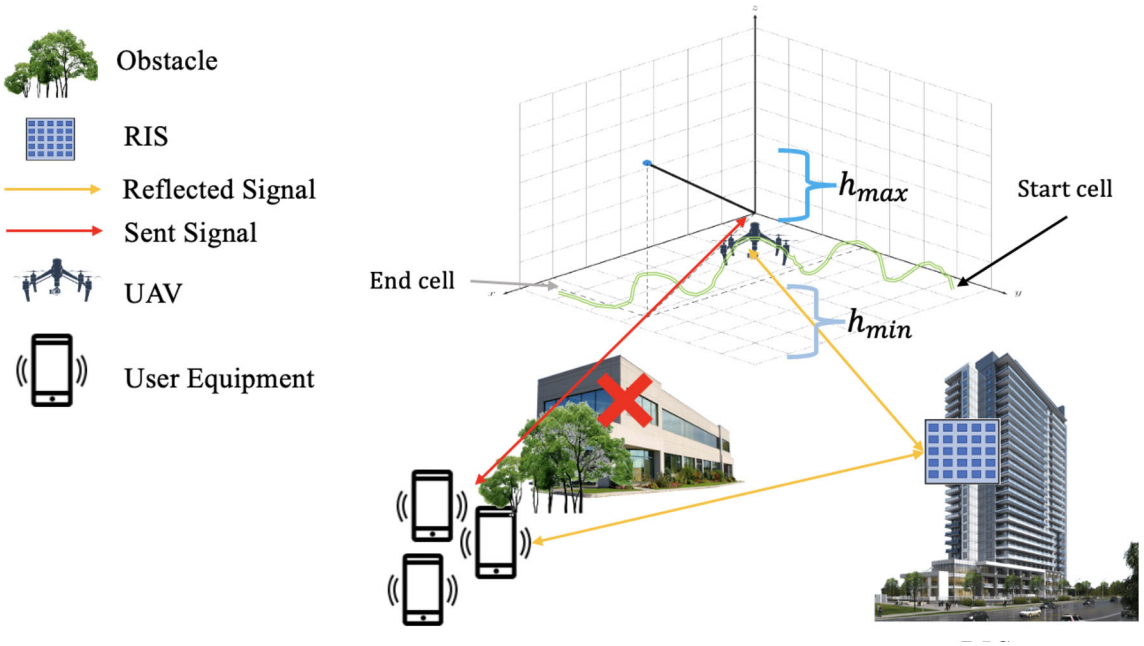

Fig. 9 3D trajectory and phase shift using U-UAV^{RIS}

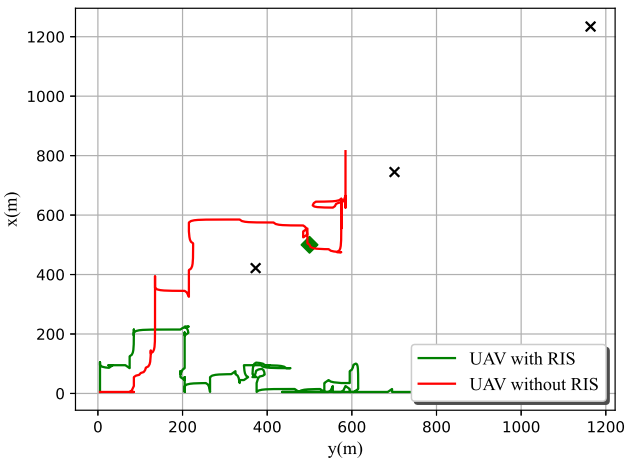

Fig. 10 Diagonal locations energy efficiency in 2D

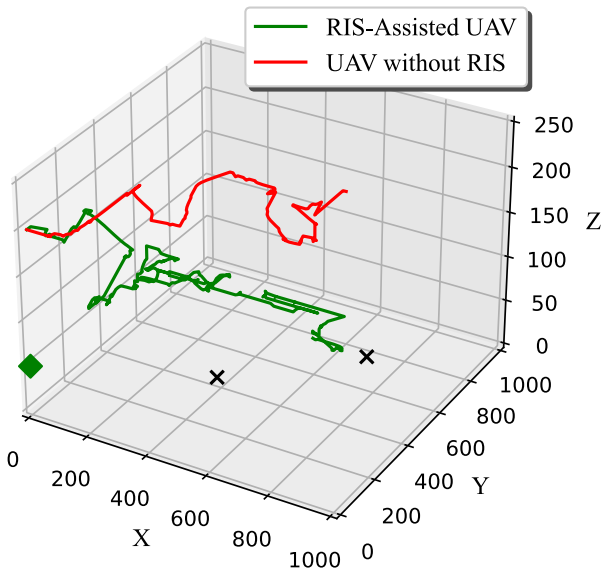

Fig. 11 Diagonal locations energy efficiency in 3D

origin. Figures 10 and 11 present two curves describing the trajectory of the UAV in two- and three-dimensional space, respectively. The red curve shows the trajectory of the UAV without RIS assistance where the UAV hovers in the same general area, only close to one set of UE. The green curve shows the UAV trajectory with RIS assistance, where the UAV hovers closer to the general area of all three UE. Figure 11 shows the height of the UAV throughout the trajectory as well.

In Fig. 12, the CDFs of the data rates are shown for the UAV without RIS assistance as the red curve and the UAV with RIS assistance as the green curve. Comparing the cumulative distribution function of both, the performance of the UAV with RIS assistance is noticeably better. In Fig. 13, the CDFs of the energy efficiency are shown for the UAV without RIS assistance as the red curve and the UAV with RIS assistance as the green curve. In this set of results, the energy efficiency attained by utilizing the RIS in the scheme is much greater and much more significant. Also, the energy saved by using an RIS is notable in this scheme.

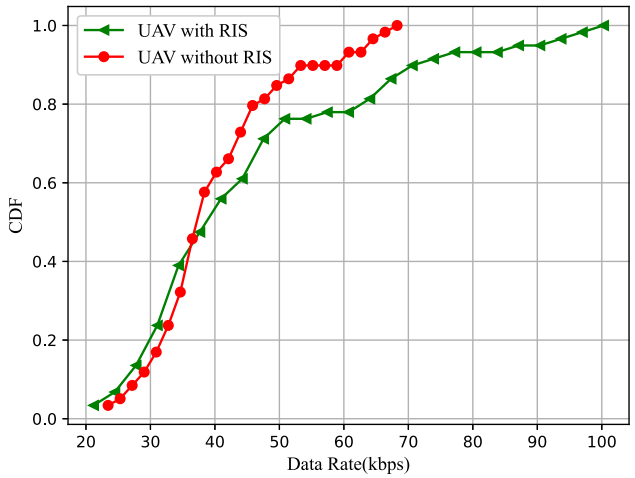

Fig. 12 UAV 3D trajectory and phase optimization data rate

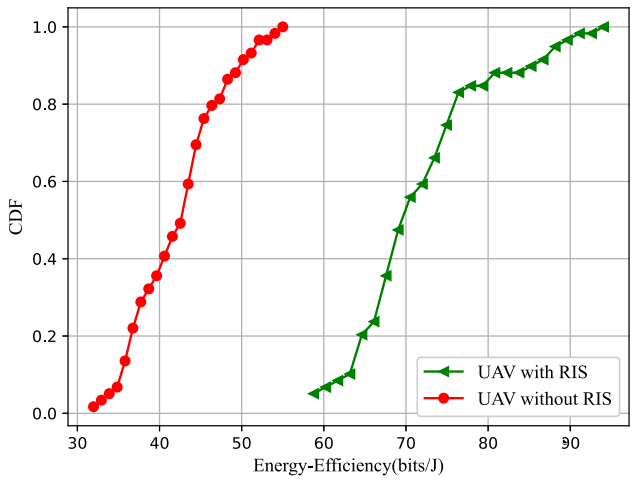

Fig. 13 UAV 3D trajectory and phase optimization energy efficiency

5 Challenges

The challenges of UAV^{RIS} applications are significant, particularly in hardware, energy efficiency, and channel information. The research challenges in these areas are discussed in this section, along with insights from the previous work summarized in this survey.

Given the nature of UAVs, researchers are concerned with the durability of mounting an RIS on a UAV. These concerns directly follow under SWaP constraints. In some cases, a direct link exists between UE and BS, and reflected signals from an RIS may not be necessary; however, this case is ideal. A direct, unblocked path may only sometimes exist, so the merger of these technologies brings a signal path with optimal quality. The challenges and constraints of bringing these solutions involve hardware, placement UAV^{RIS}, and trajectory constraints.

5.1 UAV^{RIS} Size and Weight

Constraining the number of elements when mounting an RIS on a UAV is important. A large RIS with many meta-elements requiring more than the maximum power allotted by the UAV may violate the SWaP constraints [7, 13]. These concerns are detailed in Sects. 3.1 and 3.2. One example includes leveraging processing power between the BS and RIS or the UAV and RIS. Another example is optimizing the algorithms utilized in the approaches to use fewer reflecting elements hence decreasing the weight and size of the RIS used to adhere to the UAV's respective size and weight constraints [22]. For example, the approach in [81] utilizes an RIS with 1600 elements, which adhere to the SWaP constraints of the respective approach.

The weight of the cable used to tether the T-UAV can significantly impact the UAV's performance. The weight of the tether can affect the UAV's maneuverability and stability, particularly in windy conditions, as well as its maximum altitude and speed. Therefore, it is crucial to carefully consider the weight of the cable when designing and operating a T-UAV system.

5.2 UAV^{RIS} Energy Consumption

U-UAVs are known to have a relatively limited battery life [7, 22]. For each RIS element, the dissipated power per RIS element is caused by the controller circuitry power consumption required for the adaptive phase shift [82]. The concern is whether a U-UAV's power is sufficient for the UAV and the RIS. Regarding size and weight constraints, the authors in [11, 19] optimize the UAV and RIS power consumption to extend the battery life. However, most studies on UAV^{RIS} did not consider the battery consumption of the UAV, or if it is considered, practical constraints are not considered [83].

Practical dimensions for UAV^{RIS} are presented in Tables 9 and 10. These dimensions are provided based on [27, 36, 84, 85]. The dimensions mentioned in Tables 9 and 10 are merely suggestions. Other references use different dimensions, such as [82], which uses up to 1000 RIS elements compared to 256 in Table 10. RIS supports various bandwidths and frequencies depending on how the RIS was manufactured. RIS can support anywhere from sub-6 GHz to mm-Wave frequencies to THz frequencies [41, 48].

6 Future Directions and Conclusion

It is important to consider how future solutions can be inspired by the precedent studies mentioned in this survey. This section provides insight and explores potential future directions for UAV^{RIS} research and provides concluding statements that summarize the key points of the survey.

Table 9 Example of dimensions for UAVs [27, 85]

Dimension	Fixed-wing	Multi-rotor
Size	183 cm wingspan 129 cm length	59 × 59 × 39 cm
Weight	4 kg	7.25 kg
Weight capacity	500 g	1 kg
Flight time (U-UAV)	40 mins	12 mins
Data link range	15 km	8 km
Tether length	100 m	
Tether weight	16 g/m	

Table 10 Example of RIS dimensions [36, 84]

Dimension	Suggestion
Weight	100 s of g
Number of elements	16 × 16 (256)
Size of RIS	800 × 800 mm
Size of element	6 × 6 × 2 mm^3

6.1 Future Directions

6.1.1 Direction 1: Creating Front-/Back-Haul Using T-UAV^{RIS}

T-UAV^{RIS} technology offers a promising solution to mitigate the failure of fronthaul and backhaul links in wireless communication networks. By flying at high altitudes, T-UAVs provide extensive coverage and can access challenging terrains, making them highly flexible and adaptable to dynamic communication needs [16]. Moreover, the direct link between the UAV and the BS enables the T-UAV to quickly adjust to changes in communication requirements, while its tethered design ensures unlimited flying time and reduces susceptibility to communication disruptions.

In addition to these advantages, T-UAV^{RIS} technology employs RIS to optimize wireless communication, improving the network's overall performance by reflecting signals in real time. This highly efficient and cost-effective approach eliminates the need for expensive infrastructure such as additional BSs or optical fiber, making it an attractive alternative to traditional wireless communication infrastructure [16]. Overall, T-UAV^{RIS} technology provides a reliable, efficient, and cost-effective solution to address the challenges of fronthaul and backhaul link failures in wireless communication networks.

6.1.2 Direction 2: UAV^{RIS} Secure Communications

Ground user to base station secure communications can be enhanced by using U-UAV^{RIS} technology. Deploying U-UAVs as temporary BS and sending a follower U-UAV deployed at a static location acting as a signal jammer for illegitimate users enhances secure communications. By adjusting the RIS phase shifts and the locations of the U-UAVs, the secrecy rate increases due to introducing the two technologies [60].

In this case, the RIS's phase shifts and transmit power along with the U-UAV trajectories, enhancing the average secrecy rate. This deployment scheme allows for the creation of dynamic LoS links in the secure communications network to ensure that user integrity is preserved [60].

One of the main challenges of improving secure communications through the introduction of a temporary U-UAV BS and the jammer is introducing the flexibility to respond to countermeasures from the eavesdropper and ensuring that friendly signals in the communication scheme avoid interference from the jammer [60].

6.1.3 Direction 3: STAR–RIS–UAV Communications

Simultaneously transmitting and receiving (STAR) RIS technologies have been a topic of interest for scholars due to their differences from typical RIS technologies. STAR-RIS technologies inherently transmit and receive signals on either side of the surface to achieve 360-degree wireless coverage [86]. Although this technology describes favorable results, STAR-RIS requires the design of complex signal transmission and receiving schemes to achieve the desirable results [86].

STAR-RIS can assist U-UAVs to increase coverage of the U-UAV and attain enhanced network properties such as increased robustness and optimized trajectory design with more degrees of freedom. The desirable 360-degree wireless coverage from STAR-RIS allows for full utilization of the U-UAV and allows ground users to receive communications from the non-reflective side of a conventional RIS [50]. The 360-degree coverage is adapted for high-mobility U-UAV communications while coming into contact with dynamic and random obstacles existing in the environment. As such, machine learning solutions can be introduced to increase the robustness of the approaches that utilize STAR-RIS-assisted UAV approaches and to improve the learning of the dynamic network environment [50].

6.1.4 Direction 4: Mobile Edge Computing (MEC) in 6G

The future of wireless communication networks lies in integrating emerging technologies such as MEC and RIS to meet the growing demand for high-speed and low-latency communication. In the context of 6G networks, MEC and RIS can provide significant benefits by enabling faster data processing, reducing network congestion, and enhancing communication security and privacy. One potential future direction is the development of intelligent algorithms that optimize the deployment of MEC and RIS nodes to improve

network performance and efficiency. Another direction is the exploration of new use cases that leverage the capabilities of MEC and RIS, such as real-time virtual and augmented reality applications, autonomous vehicles, and smart cities [87].

An example of a scheme for MEC and traffic-offloading uses U-UAV^{RIS} over an RF-powered 6G network. The UAV serves as an MEC server to collect data from multiple UEs, while several sets of RIS are deployed to enhance simultaneous wireless data and energy transmissions [59, 88].

Solution schemes are introduced to minimize the U-UAV's total flying time while enabling data collection and processing. This is achieved by jointly optimizing the RIS phase shifts, U-UAV's trajectory, flying time, resource allocation, and scheduling of ground users [59].

Using T-UAV^{RIS} for MEC offers several advantages over traditional MEC and traffic-offloading schemes, including greater flexibility, improved signal strength, reduced interference, and a continuous power supply. Using a U-UAV^{RIS} in this system provides a promising approach for improving communication and enabling efficient mobile-edge-computing in 6G mobile wireless networks [59, 88, 89].

6.1.5 Direction 5: UAV^{RIS} ML and AI-Driven Optimization

In order to enhance the performance of RIS-based systems, optimizing RIS phase shift matrices is critical. RISs have hundreds of reflecting elements in practical deployments, making the optimization process complex. Existing methods for phase shift design typically rely on model-based optimization, which can be computationally expensive due to the non-convexity of the phase shift constraints and objective function. However, integrating ML and/or AI into the optimization process is an appealing data-driven scheme that can extract system features without a specific mathematical model. Furthermore, using unmanned aerial vehicles (UAVs) in RIS-based systems introduces additional challenges and opportunities that warrant further research in AI-driven design and optimization, such as trajectory planning using reinforcement learning [90].

6.2 Conclusion

Many techniques have been developed to improve wireless network communications, but unexpected events such as equipment failures, natural disasters, or unforeseen blockages can still hinder communications. This highlights the need for the proposed integration of RIS and UAV technologies. Individually, these technologies are powerful solutions for addressing unexpected events, but when combined, they offer an even more powerful solution to communication problems. Using untethered and tethered UAVs with RIS can lead to innovative solutions that benefit from merging these technologies. While only a few solutions currently utilize tethered UAVs, there is clear potential for significant improvement when incorporating RIS systems. Despite challenges such as size, weight, and power (SWaP) constraints, alignment and positioning of each technology, and the common problem of choosing the correct optimization constraints, the merger of these two technologies is successful. This paper presents two case studies. The first case study demonstrates the benefit of using a UAV mounting an RIS to mitigate the effect of base station fronthaul failure in 5G and beyond networks. The second case study shows that utilizing U-UAV^{RIS} to enhance the 3D trajectory and phase shift to improve energy efficiency and the overall data rate is significant. Some future directions are also discussed to innovate in pushing these technologies toward advancing communications and wireless networking in 6G and beyond. This further emphasizes the potential for this technology integration to improve communication in unexpected events and unforeseen situations.

References

1. Zhang, Z.; Dai, L.; Chen, X.; Liu, C.; Yang, F.; Schober, R.; Poor, H.V.: Active RIS vs. passive RIS: which will prevail in 6G? IEEE Trans. Commun. **71**(3), 1707–1725 (2023). https://doi.org/10.1109/tcomm.2022.3231893
2. Hassouna, S.; Jamshed, M.A.; Rains, J.; Kazim, J.U.R.; Rehman, M.U.; Abualhayja, M.; Mohjazi, L.; Cui, T.J.; Imran, M.A.; Abbasi, Q.H.: A survey on reconfigurable intelligent surfaces: wireless communication perspective. IET Commun. **17**(5), 497–537 (2023). https://doi.org/10.1049/cmu2.12571
3. Wu, Q.; Zhang, R.: Towards smart and reconfigurable environment: intelligent reflecting surface aided wireless network. IEEE Commun. Mag. **58**(1), 106–112 (2020). https://doi.org/10.1109/MCOM.001.1900107
4. Alhamad, R.: Throughput and detection probability of interweave cognitive radio networks using intelligent reflecting surfaces. Arab. J. Sci. Eng. **47**, 3281–3292 (2022). https://doi.org/10.1007/s13369-021-06211-4
5. You, C.; Kang, Z.; Zeng, Y.; Zhang, R.: Enabling smart reflection in integrated air-ground wireless network: IRS meets UAV. IEEE Wirel. Commun. **28**(6), 138–144 (2021). https://doi.org/10.1109/MWC.001.2100148
6. Cai, G.; Dias, J.; Seneviratne, L.: A survey of small-scale unmanned aerial vehicles: recent advances and future development trends. Unmanned Syst. **02**(02), 175–199 (2014). https://doi.org/10.1142/S2301385014300017
7. Gupta, L.; Jain, R.; Vaszkun, G.: Survey of important issues in UAV communication networks. IEEE Commun. Surv. Tutor. **18**(2), 1123–1152 (2016). https://doi.org/10.1109/COMST.2015.2495297
8. Din, A.F.U.; Mir, I.; Gul, F.; et al.: Reinforced learning-based robust control design for unmanned aerial vehicle. Arab. J. Sci. Eng. **48**, 1221–1236 (2023). https://doi.org/10.1007/s13369-022-06746-0
9. Mei, H.; Yang, K.; Liu, Q.; Wang, K.: 3D-trajectory and phase-shift design for RIS-assisted UAV systems using deep reinforcement learning. IEEE Trans. Veh. Technol. **71**(3), 3020–3029 (2022). https://doi.org/10.1109/TVT.2022.3143839

10. Ben Aissa, S.; Ben Letaifa, A.: UAV communications with machine learning: challenges, applications and open issues. Arab. J. Sci. Eng. **47**(2), 1559–1579 (2022)
11. Abdalla, A.S.; Rahman, T.F.; Marojevic, V.: UAVs with reconfigurable intelligent surfaces: applications, challenges, and opportunities. arXiv, https://doi.org/10.48550/ARXIV.2012.04775 . arXiv:2012.04775 (2020)
12. Bor-Yaliniz, I.; Salem, M.; Senerath, G.; Yanikomeroglu, H.: Is 5G ready for drones: a look into contemporary and prospective wireless networks from a standardization perspective. IEEE Wirel. Commun. **26**(1), 18–27 (2019). https://doi.org/10.1109/MWC.2018.1800229
13. Pogaku, A.C.; Do, D.-T.; Lee, B.M.; Nguyen, N.D.: UAV-assisted RIS for future wireless communications: a survey on optimization and performance analysis. IEEE Access **10**, 16320–16336 (2022). https://doi.org/10.1109/ACCESS.2022.3149054
14. Zhu, Y.; Mao, B.; Kato, N.: Intelligent reflecting surface in 6g vehicular communications: a survey. IEEE Open J. Veh. Technol. **3**, 266–277 (2022). https://doi.org/10.1109/OJVT.2022.3177253
15. Selim, M.Y.; Kamal, A.E.: Post-disaster 4G/5G network rehabilitation using drones: solving battery and backhaul issues. In: 2018 IEEE Globecom Workshops (GC Wkshps), pp. 1–6 (2018). https://doi.org/10.1109/GLOCOMW.2018.8644135
16. Kishk, M.; Bader, A.; Alouini, M.-S.: Aerial base station deployment in 6G cellular networks using tethered drones: the mobility and endurance tradeoff. IEEE Veh. Technol. Mag. **15**(4), 103–111 (2020). https://doi.org/10.1109/MVT.2020.3017885
17. Bushnaq, O.M.; Kishk, M.A.; Celik, A.; Alouini, M.-S.; Al-Naffouri, T.Y.: Optimal deployment of tethered drones for maximum cellular coverage in user clusters. IEEE Trans. Wirel. Commun. **20**(3), 2092–2108 (2021). https://doi.org/10.1109/TWC.2020.3039013
18. Mozaffari, M.; Saad, W.; Bennis, M.; Nam, Y.-H.; Debbah, M.: A tutorial on UAVs for wireless networks: applications, challenges, and open problems. IEEE Commun. Surv. Tutor. **21**(3), 2334–2360 (2019). https://doi.org/10.1109/COMST.2019.2902862
19. Fotouhi, A.; Qiang, H.; Ding, M.; Hassan, M.; Giordano, L.G.; Garcia-Rodriguez, A.; Yuan, J.: Survey on UAV cellular communications: Practical aspects, standardization advancements, regulation, and security challenges. IEEE Commun. Surv. Tutor. **21**(4), 3417–3442 (2019). https://doi.org/10.1109/COMST.2019.2906228
20. Zeng, Y.; Zhang, R.; Lim, T.J.: Wireless communications with unmanned aerial vehicles: opportunities and challenges. IEEE Commun. Mag. **54**(5), 36–42 (2016). https://doi.org/10.1109/MCOM.2016.7470933
21. Ren, Q.; Abbasi, O.; Kurt, G.K.; Yanikomeroglu, H.; Chen, J.: High altitude platform station (haps) assisted computing for intelligent transportation systems. In: 2021 IEEE Global Communications Conference (GLOBECOM), pp. 1–6 (2021). https://doi.org/10.1109/GLOBECOM46510.2021.9685074
22. Alzahrani, B.; Oubbati, O.S.; Barnawi, A.; Atiquzzaman, M.; Alghazzawi, D.: UAV assistance paradigm: state-of-the-art in applications and challenges. J. Netw. Comput. Appl. **166**, 102706 (2020). https://doi.org/10.1016/j.jnca.2020.102706
23. Shi, W.; Zhou, H.; Li, J.; Xu, W.; Zhang, N.; Shen, X.: Drone assisted vehicular networks: architecture, challenges and opportunities. IEEE Netw. **32**(3), 130–137 (2018). https://doi.org/10.1109/MNET.2017.1700206
24. Shang, B.; Shafin, R.; Liu, L.: UAV swarm-enabled aerial reconfigurable intelligent surface (SARIS). IEEE Wirel. Commun. **28**(5), 156–163 (2021). https://doi.org/10.1109/MWC.010.2000526
25. Wang, J.; Jiang, C.; Han, Z.; Ren, Y.; Maunder, R.G.; Hanzo, L.: Taking drones to the next level: cooperative distributed unmanned-aerial-vehicular networks for small and mini drones. IEEE Veh. Technol. Mag. **12**(3), 73–82 (2017). https://doi.org/10.1109/MVT.2016.2645481
26. Wang, J.; Jiang, C.; Wei, Z.; Pan, C.; Zhang, H.; Ren, Y.: Joint UAV hovering altitude and power control for space-air-ground IoT networks. IEEE Internet Things J. **6**(2), 1741–1753 (2019). https://doi.org/10.1109/JIOT.2018.2875493
27. Boon, M.A.; Drijfhout, A.P.; Tesfamichael, S.: Comparison of a fixed-wing and multi-rotor UAV for environmental mapping applications: a case study. ISPRS Int. Arch. Photogramm. Remote Sens. Spat. Inf. Sci. **42W6**, 47–54 (2017). https://doi.org/10.5194/isprs-archives-XLII-2-W6-47-2017
28. Thamm, F.-P.; Brieger, N.; Neitzke, K.-P.; Meyer, M.; Jansen, R.; Mönninghof, M.: Songbird—an innovative UAS combining the advantages of fixed wing and multi rotor UAS. ISPRS Int. Arch. Photogramm. Remote Sens. Spat. Inf. Sci. **XL–1/W4**, 345–349 (2015). https://doi.org/10.5194/isprsarchives-XL-1-W4-345-2015
29. Hybrid VTOL fixed wing UAV manufacturers: VTOL fixed wing drones (2022). https://www.unmannedsystemstechnology.com/expo/hybrid-vtol-fixed-wing-uav-manufacturers/
30. Albatross UAV : Bvlos Drone. https://www.appliedaeronautics.com/
31. Press, Mortimer, G.: Kargu Rotary Wing Attack Drone (2020). https://www.suasnews.com/2020/11/kargu-rotary-wing-attack-drone/
32. Belmekki, B.E.Y.; Alouini, M.-S.: Unleashing the potential of networked tethered flying platforms: prospects, challenges, and applications. IEEE Open J. Veh. Technol. **3**, 278–320 (2022). https://doi.org/10.1109/OJVT.2022.3177946
33. Mahmood, K.; Ismail, N.A.; Suhadis, N.M.: Tethered aerostat envelope design and applications: a review. AIP Conf. Proc. **2226**(1), 050003 (2020). https://doi.org/10.1063/5.0002358
34. Selim, M.Y.; Alsharoa, A.; Kamal, A.E.: Short-term and long-term cell outage compensation using UAVs in 5G networks. In: 2018 IEEE Global Communications Conference (GLOBECOM), pp. 1–6 (2018). https://doi.org/10.1109/GLOCOM.2018.8648054
35. Kumaravelu, V.B.; Jadhav, H.K.; Anjana, B.S.; Gudla, V.V.; Murugadass, A.; Imoize, A.L.: In: Imoize, A.L., Islam, S.M.N., Poongodi, T., Ramasamy, L.K., Siva Prasad, B.V.V. (eds.) Unmanned Aerial Vehicle-Assisted Reconfigurable Intelligent Surface for Energy Efficient and Reliable Communication, pp. 173–201. Springer, Cham (2023). https://doi.org/10.1007/978-3-031-08395-2_8
36. Li, L.; Jun Cui, T.; Ji, W.; Liu, S.; Ding, J.; Wan, X.; Bo Li, Y.; Jiang, M.; Qiu, C.-W.; Zhang, S., et al.: Electromagnetic reprogrammable coding-metasurface holograms. Nature Publishing Group (2017). https://www.nature.com/articles/s41467-017-00164-9
37. Renzo, M.D.; Debbah, M.; Phan-Huy, D.-T.; Zappone, A.; Alouini, M.-S.; Yuen, C.; Sciancalepore, V.; Alexandropoulos, G.C.; Hoydis, J.; Gacanin, H.; Rosny, J.; Bounceu, A.; Lerosey, G.; Fink, M.: Smart radio environments empowered by AI reconfigurable meta-surfaces: an idea whose time has come (2019)
38. Sievenpiper, D.F.; Schaffner, J.H.; Song, H.J.; Loo, R.Y.; Tangonan, G.: Two-dimensional beam steering using an electrically tunable impedance surface. IEEE Trans. Antennas Propag. **51**(10), 2713–2722 (2003). https://doi.org/10.1109/TAP.2003.817558
39. Holloway, C.L.; Mohamed, M.A.; Kuester, E.F.; Dienstfrey, A.: Reflection and transmission properties of a metafilm: with an application to a controllable surface composed of resonant particles. IEEE Trans. Electromagn. Compat. **47**(4), 853–865 (2005). https://doi.org/10.1109/TEMC.2005.853719
40. Liang, Y.-C.; Chen, J.; Long, R.; He, Z.-Q.; Lin, X.; Huang, C.; Liu, S.; Shen, X.S.; Di Renzo, M.: Reconfigurable Intelligent Surfaces for Smart Wireless Environments: Channel Estimation, System Design and Applications in 6G Networks—Science China Infor-

mation Sciences. Science China Press (2021). https://link.springer.com/article/10.1007/s11432-020-3261-5
41. Zhang, Q.; Saad, W.; Bennis, M.: Reflections in the sky: millimeter wave communication with UAV-carried intelligent reflectors. In: 2019 IEEE Global Communications Conference (GLOBECOM), pp. 1–6 (2019). https://doi.org/10.1109/GLOBECOM38437.2019.9013626
42. Lu, H.; Zeng, Y.; Jin, S.; Zhang, R.: Enabling panoramic full-angle reflection via aerial intelligent reflecting surface (2020)
43. Ndjiongue, A.R.; Ngatched, T.M.N.; Dobre, O.A.; Armada, A.G.; Haas, H.: Analysis of RIS-based terrestrial-FSO link over g-g turbulence with distance and jitter ratios. J. Lightw. Technol. **39**(21), 6746–6758 (2021). https://doi.org/10.1109/JLT.2021.3108532
44. Cao, X.; Yang, B.; Huang, C.; Yuen, C.; Renzo, M.D.; Niyato, D.; Han, Z.: Reconfigurable intelligent surface-assisted aerial-terrestrial communications via multi-task learning. IEEE J. Sel. Areas Commun. **39**(10), 3035–3050 (2021). https://doi.org/10.1109/JSAC.2021.3088634
45. Long, R.; Liang, Y.-C.; Pei, Y.; Larsson, E.G.: Active reconfigurable intelligent surface-aided wireless communications. IEEE Trans. Wirel. Commun. **20**(8), 4962–4975 (2021). https://doi.org/10.1109/TWC.2021.3064024
46. Zhou, T.; Xu, K.; Shen, Z.; Xie, W.; Zhang, D.; Xu, J.: AOA-based positioning for aerial intelligent reflecting surface-aided wireless communications: an angle-domain approach. IEEE Wirel. Commun. Lett. **11**(4), 761–765 (2022). https://doi.org/10.1109/LWC.2022.3143099
47. Nguyen-Kha, H.; Nguyen, H.V.; Le, M.T.P.; Shin, O.-S.: Joint UAV placement and IRS phase shift optimization in downlink networks. IEEE Access **10**, 111221–111231 (2022). https://doi.org/10.1109/ACCESS.2022.3214663
48. Abuzainab, N.; Alrabeiah, M.; Alkhateeb, A.; Sagduyu, Y.E.: Deep learning for thz drones with flying intelligent surfaces: Beam and handoff prediction. In: 2021 IEEE International Conference on Communications Workshops (ICC Workshops), pp. 1–6 (2021). https://doi.org/10.1109/ICCWorkshops50388.2021.9473804
49. Truong, T.P.; Tuong, V.D.; Dao, N.-N.; Cho, S.: Flyreflect: joint flying IRS trajectory and phase shift design using deep reinforcement learning. IEEE Internet Things J. **10**(5), 4605–4620 (2023). https://doi.org/10.1109/JIOT.2022.3218740
50. Zhao, J.; Zhu, Y.; Mu, X.; Cai, K.; Liu, Y.; Hanzo, L.: Simultaneously transmitting and reflecting reconfigurable intelligent surface (STAR-RIS) assisted UAV communications. IEEE J. Sel. Areas Commun. **40**(10), 3041–3056 (2022). https://doi.org/10.1109/JSAC.2022.3196102
51. Pan, Y.; Wang, K.; Pan, C.; Zhu, H.; Wang, J.: UAV-assisted and intelligent reflecting surfaces-supported terahertz communications. IEEE Wirel. Commun. Lett. **10**(6), 1256–1260 (2021). https://doi.org/10.1109/LWC.2021.3063365
52. Yao, Y.; Lv, K.; Ma, N.; Yue, X.; Qin, X.; Yun, X.: Energy efficient air-to-ground communication networks with reconfigurable intelligent surface. J. Commun. Netw. **24**(5), 555–565 (2022). https://doi.org/10.23919/JCN.2022.000025
53. Li, Z.; Chen, W.; Cao, H.; Tang, H.; Wang, K.; Li, J.: Joint communication and trajectory design for intelligent reflecting surface empowered UAV SWIPT networks. IEEE Trans. Veh. Technol. **71**(12), 12840–12855 (2022). https://doi.org/10.1109/TVT.2022.3196039
54. Ren, H.; Zhang, Z.; Peng, Z.; Li, L.; Pan, C.: Energy minimization in RIS-assisted UAV-enabled wireless power transfer systems. IEEE Internet Things J. (2022). https://doi.org/10.1109/JIOT.2022.3150178
55. Heimann, K.; Sliwa, B.; Patchou, M.; Wietfeld, C.: Modeling and simulation of reconfigurable intelligent surfaces for hybrid aerial and ground-based vehicular communications (2021)
56. Eskandari, M.; Savkin, A.V.; Ni, W.: Consensus-based autonomous navigation of a team of RIS-equipped UAVs for los wireless communication with mobile nodes in high-density areas. IEEE Trans. Autom. Sci. Eng. (2022). https://doi.org/10.1109/TASE.2022.3183335
57. Nguyen, M.-H.T.; Garcia-Palacios, E.; Do-Duy, T.; Dobre, O.A.; Duong, T.Q.: UAV-aided aerial reconfigurable intelligent surface communications with massive MIMO system. IEEE Trans. Cogn. Commun. Netw. **8**(4), 1828–1838 (2022). https://doi.org/10.1109/TCCN.2022.3187098
58. Mei, H.; Yang, K.; Liu, Q.; Wang, K.: 3d-trajectory and phase-shift design for RIS-assisted UAV systems using deep reinforcement learning. IEEE Trans. Veh. Technol. **71**(3), 3020–3029 (2022). https://doi.org/10.1109/TVT.2022.3143839
59. Wang, F.; Zhang, X.: IRS/UAV-based edge-computing/traffic-offloading over RF-powered 6G mobile wireless networks. In: 2022 IEEE Wireless Communications and Networking Conference (WCNC), pp. 1272–1277 (2022). https://doi.org/10.1109/WCNC51071.2022.9771971
60. Guo, J.; Yu, L.; Chen, Z.; Yao, Y.; Wang, Z.; Wang, Z.; Zhao, Q.: RIS-assisted secure UAV communications with resource allocation and cooperative jamming. IET Commun. **16**(13), 1582–1592 (2022). https://doi.org/10.1049/cmu2.12416
61. Quispe, J.J.L.; Maciel, T.F.; Silva, Y.C.B.; Klein, A.: Joint beamforming and BS selection for energy-efficient communications via aerial-RIS. In: 2021 IEEE Globecom Workshops (GC Wkshps), pp. 1–6 (2021). https://doi.org/10.1109/GCWkshps52748.2021.9681981
62. Mu, X.; Liu, Y.; Guo, L.; Lin, J.; Poor, H.V.: Intelligent reflecting surface enhanced multi-UAV NOMA networks. IEEE J. Sel. Areas Commun. **39**(10), 3051–3066 (2021). https://doi.org/10.1109/JSAC.2021.3088679
63. Li, S.; Duo, B.; Renzo, M.D.; Tao, M.; Yuan, X.: Robust secure UAV communications with the aid of reconfigurable intelligent surfaces. IEEE Trans. Wirel. Commun. **20**(10), 6402–6417 (2021). https://doi.org/10.1109/TWC.2021.3073746
64. Badarneh, O.S.; Awad, M.K.; Muhaidat, S.; Almehmadi, F.S.: Performance analysis of intelligent reflecting surface-aided decode-and-forward UAV communication systems. IEEE Syst. J. **17**(1), 246–257 (2023). https://doi.org/10.1109/JSYST.2022.3178327
65. Nguyen, M.D.; Le, L.B.; Girard, A.: UAV placement and resource allocation for intelligent reflecting surface assisted UAV-based wireless networks. IEEE Commun. Lett. **26**(5), 1106–1110 (2022). https://doi.org/10.1109/LCOMM.2022.3149467
66. Tian, K.; Chi, Y.; Duo, B.; Yuan, X.: Hybrid offline-online design for reconfigurable intelligent surface aided UAV communication. IEEE Commun. Lett. **27**(5), 1372–1376 (2023). https://doi.org/10.1109/LCOMM.2023.3255241
67. Boulogeorgos, A.-A.A.; Alexiou, A.; Renzo, M.D.: Outage performance analysis of RIS-assisted UAV wireless systems under disorientation and misalignment. IEEE Trans. Veh. Technol. **71**(10), 10712–10728 (2022). https://doi.org/10.1109/TVT.2022.3187050
68. Fang, S.; Chen, G.; Li, Y.: Joint optimization for secure intelligent reflecting surface assisted UAV networks. IEEE Wirel. Commun. Lett. **10**(2), 276–280 (2021). https://doi.org/10.1109/LWC.2020.3027969
69. Khalil, A.A.; Selim, M.Y.; Rahman, M.A.: CURE: enabling RF energy harvesting using cell-free massive MIMO UAVs assisted by RIS (2021)
70. Belmekki, B.E.Y.; Alouini, M.-S.: Unleashing the potential of networked tethered flying platforms: prospects, challenges, and applications. IEEE Open J. Veh. Technol. **3**, 278–320 (2022). https://doi.org/10.1109/OJVT.2022.3177946
71. Bhowal, A.; Aïssa, S.: RIS-aided communications in indoor and outdoor environments: performance analysis with a realistic chan-

nel model. IEEE Trans. Veh. Technol. **71**(12), 13356–13360 (2022). https://doi.org/10.1109/TVT.2022.3143841
72. Alexandropoulos, G.C.; Shlezinger, N.; Hougne, P.: Reconfigurable intelligent surfaces for rich scattering wireless communications: recent experiments, challenges, and opportunities. IEEE Commun. Mag. **59**(6), 28–34 (2021). https://doi.org/10.1109/MCOM.001.2001117
73. Saigre-Tardif, C.; Hougne, P.D.: A self-adaptive RIS that estimates and shapes fading rich-scattering wireless channels. In: 2022 IEEE 95th Vehicular Technology Conference: (VTC2022-Spring). IEEE (2022). https://doi.org/10.1109/vtc2022-spring54318.2022.9860667 .
74. Beaulieu, N.C.; Jiandong, X.: A novel fading model for channels with multiple dominant specular components. IEEE Wirel. Commun. Lett. **4**(1), 54–57 (2015). https://doi.org/10.1109/LWC.2014.2367501
75. Kansal, V.; Singh, S.: Analysis of effective capacity over Beaulieu-Xie fading model. In: 2017 IEEE International WIE Conference on Electrical and Computer Engineering (WIECONECE), pp. 207–210 (2017). https://doi.org/10.1109/WIECONECE.2017.8468917
76. Bjornson, E.: intelligent reflecting surface vs. decode-and-forward: how large surfaces are needed to beat relaying? https://github.com/emilbjornson/IRS-relaying
77. Further advancements for E-UTRA physical layer aspects (Release 9) (2010). https://portal.3gpp.org/desktopmodules/Specifications/SpecificationDetails.aspx?specificationId=2493
78. He, Z.-Q.; Yuan, X.: Cascaded channel estimation for large intelligent metasurface assisted massive MIMO. IEEE Wirel. Commun. Lett. **9**(2), 210–214 (2020). https://doi.org/10.1109/LWC.2019.2948632
79. Taha, A.; Alrabeiah, M.; Alkhateeb, A.: Deep learning for large intelligent surfaces in millimeter wave and massive MIMO systems. In: 2019 IEEE Global Communications Conference (GLOBECOM), pp. 1–6 (2019). https://doi.org/10.1109/GLOBECOM38437.2019.9013256
80. Haibo, M.: 3D-trajectory and phase-shift design for RIS-assisted UAV systems using deep reinforcement learning. https://github.com/HaiboMei/UAV-RIS-DRL/
81. Bie, Q.; Liu, Y.; Wang, Y.; Zhao, X.; Zhang, X.Y.: Deployment optimization of reconfigurable intelligent surface for relay systems. IEEE Trans. Green Commun. Netw. **6**(1), 221–233 (2022). https://doi.org/10.1109/TGCN.2022.3145026
82. Selim, M.Y.; Kamal, A.E.; Nait-Abdesselam, F.: X-haul outage compensation in 5G/6G using reconfigurable intelligent surfaces. In: 2022 International Telecommunications Conference (ITC-Egypt), pp. 1–6 (2022). https://doi.org/10.1109/ITC-Egypt55520.2022.9855706
83. Abeywickrama, H.V.; Jayawickrama, B.A.; He, Y.; Dutkiewicz, E.: Comprehensive energy consumption model for unmanned aerial vehicles, based on empirical studies of battery performance. IEEE Access **6**, 58383–58394 (2018). https://doi.org/10.1109/ACCESS.2018.2875040
84. Dai, L.; Wang, B.; Wang, M.; Yang, X.; Tan, J.; Bi, S.; Xu, S.; Yang, F.; Chen, Z.; Renzo, M.D.; Chae, C.-B.; Hanzo, L.: Reconfigurable intelligent surface-based wireless communications: antenna design, prototyping, and experimental results. IEEE Access **8**, 45913–45923 (2020). https://doi.org/10.1109/ACCESS.2020.2977772
85. Tethered drone systems: Tethered UAV & tethering stations: Elistair (2023). https://www.unmannedsystemstechnology.com/company/elistair/
86. Ahmed, M.; Wahid, A.; Laique, S.S.; Khan, W.U.; Ihsan, A.; Xu, F.; Chatzinotas, S.; Han, Z.: A survey on star-RIS: use cases, recent advances, and future research challenges. IEEE Internet Things J. (2023). https://doi.org/10.1109/JIOT.2023.3279357
87. Mahbub, M.; Shubair, R.M.: IRS for multi-access edge computing in 6G networks. arXiv preprint arXiv:2206.05290 (2022)
88. Pan, C.; Ren, H.; Wang, K.; Kolb, J.F.; Elkashlan, M.; Chen, M.; Renzo, M.D.; Hao, Y.; Wang, J.; Swindlehurst, A.L.; You, X.; Hanzo, L.: Reconfigurable intelligent surfaces for 6G systems: principles, applications, and research directions. IEEE Commun. Mag. **59**(6), 14–20 (2021)
89. Laroui, M.; Moungla, H.; Afifi, H.; Selim, M.Y.; Kamal, A.E.: Intelligent reflecting surface aided vehicular edge computing. In: GLOBECOM 2022—2022 IEEE Global Communications Conference, pp. 5577–5582 (2022). https://doi.org/10.1109/GLOBECOM48099.2022.10000899
90. Shahjalal, M.; Kim, W.; Khalid, W.; Moon, S.; Khan, M.; Liu, S.; Lim, S.; Kim, E.; Yun, D.-W.; Lee, J.; Lee, W.-C.; Hwang, S.-H.; Kim, D.; Lee, J.-W.; Yu, H.; Sung, Y.; Jang, Y.M.: Enabling technologies for ai empowered 6g massive radio access networks. ICT Express (2022). https://doi.org/10.1016/j.icte.2022.07.002

Springer Nature or its licensor (e.g. a society or other partner) holds exclusive rights to this article under a publishing agreement with the author(s) or other rightsholder(s); author self-archiving of the accepted manuscript version of this article is solely governed by the terms of such publishing agreement and applicable law.